

**Title:**

**An improved estimate for the  $\delta^{13}\text{C}$  and  $\delta^{18}\text{O}$  signatures of carbon monoxide produced from atmospheric oxidation of volatile organic compounds**

**5 Authors:**

\*Isaac J Vimont<sup>1,2,3</sup>, Jocelyn C. Turnbull<sup>3,4</sup>, Vasilii V. Petrenko<sup>5</sup>, Philip F. Place<sup>5</sup>, Colm Sweeney<sup>2</sup>, Natasha Miles<sup>6</sup>, Scott Richardson<sup>6</sup>, Bruce H. Vaughn<sup>1</sup>, James W.C. White<sup>1</sup>

- 10 1. Institute of Arctic and Alpine Research, Boulder, CO USA  
2. National Oceanic and Atmospheric Administration, Global Monitoring Division, Boulder, CO USA  
3. CIRES, University of Colorado, Boulder, CO, USA  
4. GNS Science, Lower Hutt, New Zealand  
5. University of Rochester Earth and Environmental Science Department, Rochester, NY, USA  
15 6. Pennsylvania State University, College Station, PA USA

\* Corresponding Author: [Isaac.vimont@colorado.edu](mailto:Isaac.vimont@colorado.edu)

**Abstract:**

20 Atmospheric carbon monoxide (CO) is a key player in global atmospheric chemistry and a regulated pollutant in urban areas. Oxidation of volatile organic compounds (VOCs) is an important component of the global CO budget and has also been hypothesized to contribute substantially to the summertime urban CO budget. In principle, stable isotopic analysis of  
25 CO could constrain the magnitude of this source. However, the isotopic signature of VOC-produced CO has not been well quantified, especially for the oxygen isotopes. We performed measurements of CO stable isotopes on air samples from two sites around Indianapolis, USA over three summers to investigate the isotopic signature of VOC-produced CO. One of the sites is located upwind of the city, allowing us to quantitatively remove the background air signal and isolate the urban CO enhancements as well as the  
30 isotopic signature of these enhancements. In addition, we use measurements of  $\Delta^{14}\text{CO}_2$  in combination with the CO:CO<sub>2</sub> emission ratio from fossil fuels to constrain the fossil fuel-

derived CO and thereby isolate the VOC-derived component of the CO enhancement. Combining these measurements and analyses, we are able to determine the carbon and oxygen isotopic signatures of CO derived from VOC oxidation as  $-32.8\text{‰} \pm 0.5\text{‰}$  and  $3.6\text{‰} \pm 1.2\text{‰}$ , respectively. Additionally, we analyzed CO stable isotopes for one year at Beech Island, South Carolina, USA, a site thought to have large VOC-derived contributions to the summertime CO budget. The Beech Island results are consistent with isotopic signatures of VOC-derived CO determined from the Indianapolis data. This study represents the first direct determination of the isotopic signatures of VOC-derived CO and will allow for improved use of isotopes in constraining the global and regional CO budgets.

10

## 1. Introduction

The global carbon monoxide (CO) budget, along with regional and local CO budgets, remain uncertain (e.g. Holloway et al., 2000; Duncan et al., 2007; Granier et al., 2011; Zhou et al., 2017; Strode et al., 2018). CO stable isotope measurements can aid in the partitioning of the sources of CO, and hence improve global and regional budgets (e.g. Brenninkmeijer et al., 1999). Several studies have incorporated stable isotopes of CO to independently constrain the sources of CO (Manning et al., 1997; Bergamaschi et al., 2000; Park et al., 2015). On the global scale, carbon monoxide (CO) has four major sources which include biomass/biofuel burning, oxidation of methane (CH<sub>4</sub>), the incomplete combustion of fossil fuels and the oxidation of volatile organic compounds (VOCs) (Logan et al., 1981; Duncan et al., 2007; Table 1). These sources are balanced by the oxidation of CO by the hydroxyl radical (OH) and a small soil sink, resulting in a residence time of CO in the atmosphere that is  $\approx 2$  months on average but varies by location and time of year (Logan et al., 1981; Duncan et al., 2007). Each CO source has a unique isotopic signature which is determined by the isotopic signature of the source material (e.g., CH<sub>4</sub>) and the process(es) by which the CO is formed. The carbon isotopic signature of methane-derived CO is much more negative than that of the other sources, largely due to the depleted carbon isotopic signature of methane (Table 1, Brenninkmeijer et al., 1999). The oxygen isotopic signature can help distinguish between combustion (fossil fuel and biomass burning) and oxidation sources (methane and

30

VOC-derived CO), with combustion sources having more positive isotopic values than oxidation sources (Table 1, Brenninkmeijer et al., 1999).

5 The isotopic signatures of CO from fossil fuel combustion and biomass burning have been relatively well quantified (Table 1). The  $^{13}\text{C}$ CO produced by oxidation of methane has also been well quantified, although the  $\text{C}^{18}\text{O}$  signature remains more uncertain (Brenninkmeijer et al., 1999). However the isotopic signatures of CO produced by the oxidation of volatile organic compounds (VOCs) remain poorly known (Brenninkmeijer and Röckmann (1997), Brenninkmeijer et al. (1999), and Gros et al. (2001). The carbon isotopic signature of CO  
10 produced by oxidation of VOCs has been estimated to around -32‰, from atmospheric measurements (Stevens and Wagner, 1989) and through analysis of the isotopic signature of isoprene, accounting for fractionation during the oxidation reaction (Sharkey et al., 1991; Conny and Currie, 1996, Conny et al., 1997).

15 Only two prior studies have tried to estimate the oxygen isotopic signature of VOC-derived CO, yielding very different values: 0‰ (Brenninkmeijer and Röckmann, 1997) or 15‰ (Stevens and Wagner, 1989), with a reported uncertainty of “greater than 3‰” (e.g. Gros et al., 2001; Table 1). As VOC oxidation is a major source of CO on global and regional scales (e.g. Logan et al., 1981; Guenther et al., 1995; Duncan et al., 2007), the large uncertainty in  
20 the associated isotopic signatures presents a major obstacle to using isotopes in investigations of the atmospheric CO budget.

Our study uses a new set of measurements to evaluate the carbon and oxygen isotopic signatures of CO produced from VOCs by analyzing the urban CO isotopic enhancements at  
25 Indianapolis, IN, USA. An urban setting for determining the isotopic signature of CO from oxidized VOCs may not seem like an obvious choice, because of the large CO enhancements from fossil fuel burning (EPA, 2014, Mak and Kra, 1999; Popa et al., 2014; Turnbull et al., 2015; Vimont et al., 2017; Turnbull et al., 2018). However, previous literature suggests that during the summer months there may also be a large urban source of CO from the  
30 oxidation of VOCs, likely from biogenic sources (Guenther et al., 1993, 1995; Carter and

Atkinson, 1996; Kanakidou and Crutzen, 1999; Cheng et al., 2017, Turnbull et al. (2006) Miller et al. (2012))

Some of these studies aimed to quantify fossil fuel CO<sub>2</sub> enhancements (CO<sub>2FF</sub>) by using CO enhancements as a proxy measurement but noted that the ratio of CO:CO<sub>2FF</sub> enhancements  
5 was higher in the summer than the winter at several sites in the eastern United States (Turnbull et al., 2006; Miller et al., 2012). A higher CO:CO<sub>2FF</sub> ratio is inconsistent with a stronger sink process such as an increase in OH during the summer months. Instead, a seasonal increase in a non-fossil fuel source provides the most likely explanation for the increase in the CO:CO<sub>2FF</sub> ratio. These studies hypothesized, but could not confirm, that  
10 oxidation of VOCs may be the source of this summertime increase in CO:CO<sub>2FF</sub> ratio.

Studies that model the effect of CO sources on the measured CO mole fraction have also indicated that oxidation of VOCs (particularly from biogenic sources) contributes significantly to the global and regional CO budget (e.g. Kanakidou and Crutzen, 1999).  
15 Isoprene and terpene emissions from broadleaf species have been shown to be a large source of VOCs (Guenther et al., 1995; Helmig et al., 1998; Harley et al., 1999), particularly in the southeastern United States (e.g. Chameides et al., 1988). Griffin et al. (2007) used the Caltech Atmospheric Chemistry Mechanism to investigate CO production by VOC oxidation at a regional scale in the United States. Their model determined that VOC oxidation could  
20 provide as much as 10-20% of the CO observed in parts of New England, but in a heavily polluted region such as the Los Angeles Basin, the percentage was much lower, on the order of 1% or less. Cheng et al. (2017) measured O<sub>3</sub> and CO mole fractions and then modeled CO production from the various sources using O<sub>3</sub>-to-CO ratios. Their model suggested the oxidation of isoprene might equal or exceed the total anthropogenic  
25 production of CO within the urban region of Baltimore, USA.

This study focuses mainly on measurements from the Indianapolis FLUX project (INFLUX). INFLUX provides a sampling methodology that allows for quantitative removal of background air signals, which isolates the urban enhancement, and simplifies the source  
30 and sink budget analysis (Turnbull et al., 2015; Vimont et al., 2017; Turnbull et al., 2018). Measurements are made not only at tower sites within and downwind of the city, but also

directly upwind of the city, so that the changes in CO mole fraction and isotopic values due to the urban influence can be isolated. The short transit time of air across the city means that removal of CO by OH (and the associated impact on the isotopic signature) can be ignored. Methane oxidation is similarly minimal in the short transit time, and biomass  
5 burning is known to be very small within the urban confines.

In addition to the CO mole fraction and stable isotopic measurements,  $^{14}\text{CO}_2$  measurements were also performed on the INFLUX samples, allowing for accurate quantification of  $\text{CO}_{2\text{FF}}$  (Turnbull et al., 2015). This allowed us to partition the urban CO enhancement between  
10 fossil fuel and VOC-derived sources. We were then able to isolate the carbon and oxygen isotopic signatures of CO produced from VOC oxidation.

To further examine our estimates of the isotopic signatures of CO produced from oxidized VOCs, we analyzed bi-monthly samples from a site at Beech Island, South Carolina, USA.  
15 This site is heavily forested and the CO mole fraction at this site should be strongly influenced by isoprene oxidation during the summer. By analyzing the isotopic signatures at this site, we were able to compare the Beech Island isotopic signals to our estimates for VOC-derived CO.

## 20 **2. Methods**

### *2.1 Tower Sampling at Indianapolis*

Indianapolis, Indiana is a metropolitan area of over one million people in the Mid-West  
25 region of the United States. It is surrounded by mostly agricultural land, interspersed with trees and foliage. Broadleaf and deciduous foliage comprises approximately 25-100% of the vegetative cover, both inside and outside of Indianapolis' borders (Figure 1, Guenther et al. (2012), Figure S1). It has hot summers (25 to 30° C) and cold winters (-8 to 1° C) that result in a distinct growing season, with the winter being relatively devoid of biogenic  
30 fluxes of CO and  $\text{CO}_2$  (Turnbull et al., 2015). INFLUX aims to develop and assess methods

for determining urban greenhouse gas emissions. CO, though not a primary greenhouse gas, is measured and used as a tracer for fossil fuel CO<sub>2</sub> emissions and to provide information for source attribution.

5 INFLUX has twelve instrumented towers within and around the urban boundary (Miles et al., 2017). The flask-sampling regime was described in detail by Vimont et al. (2017) and Turnbull et al. (2015). In brief, discrete hourly-integrated air samples are collected at six of the towers, although the integrated samplers (Turnbull et al., 2012) are moved between the twelve towers occasionally. Three of the towers have had continuous flask samples and  
10 were sampled for CO isotopes (towers 1-3, Turnbull et al., 2015; Miles et al., 2017; Turnbull et al., 2019) approximately six days per month, during the early afternoon when the strongest boundary layer mixing occurs (19:00 UTC, 14:00 local). Stable isotope measurements of CO were made on samples collected from July 2013 to July 2015. In this paper, we consider only the summer samples that were collected in July and August 2013,  
15 May-August 2014, and May – July 2015 (inclusive) from tower 1 (121 m above ground level (AGL), 39.5805° N, 86.4207° W), and tower 2 (136 m AGL, 39.7978° N, 86.0183° W) (Figure 1). The winter samples were examined in a previous study (Vimont et al., 2017) that determined in winter, CO enhancements in Indianapolis are primarily derived from fossil fuel combustion; the CO isotopic signature of the fossil fuel combustion source was also  
20 constrained. Though summer samples were also collected at tower 3 (39.7833° N, 86.1652° W), its proximity to Indianapolis' downtown district and its lower elevation above the ground (54 m AGL) meant that the signals there were strongly dominated by fossil fuel combustion sources, even in summer. Tower 2, located to the east of the urban region, was the ideal candidate for determining the isotopic signature of the oxidized VOC  
25 source of CO. Tower 2 “sees” a more mixed signal of urban and suburban sources including both fossil fuel sources and the influence of the substantial suburban vegetation (Turnbull et al., 2015; Turnbull et al., 2018).

For the samples in this study, collection was done when the wind was approximately from  
30 the west, so that Tower 1 provides a clean-air background for the towers further to the east (Turnbull et al., 2012). Tower 2 is east of the city, with only a small residential influence

and one major highway nearby, with significant foliage within its influence footprint (Turnbull et al., 2015). The distance between towers 1 and 2 is 51 km, and the average wind speed during the period sampled for this study was  $4.4 \text{ m s}^{-1}$ , which results in an average transit time of air from tower 1 to tower 2 of 3.2 hours.

5

The air samples were collected in Portable Flask Packages (PFP's) provided by the National Oceanic and Atmospheric Administration Global Reference Network (NOAA GRN)(<https://www.esrl.noaa.gov/gmd/ccgg/aircraft/sampling.html>). One-hour integrated samples were collected; this sampling regime allows for smoothing of very short-term variability that may be difficult to interpret (Turnbull et al., 2012). NOAA's Earth System Research Laboratory (ESRL) provides the infrastructure and logistical support for these PFP's, and the CO mole fraction measurements used in this study (Novelli et al., 2003).  $^{14}\text{CO}_2$  measurements were performed at GNS Science with support from University of Colorado INSTAAR (Turnbull et al., 2015).

15

## *2.2 Tower Sampling at Beech Island, South Carolina*

Beech Island, South Carolina, USA ( $33.4057^\circ\text{N}$ ,  $81.8334^\circ\text{W}$ ) is a tall tower (305m AGL) site in the NOAA Global Greenhouse Gas Reference Network (GGGRN). The Beech Island sampling site is located approximately 5.5 km from the town of Beech Island, in a sparsely populated region of South Carolina. The climate is temperate with annual temperature varying between  $6^\circ\text{C}$  and  $28^\circ\text{C}$  (NOAA Center for Environmental Information, <https://www.ncdc.noaa.gov/>). The town of Beech Island has a population of approximately 8,500, and the surrounding region population density is about 150 people per square mile (US Census Bureau, [www.census.gov](http://www.census.gov)). However, the sampling site is 15.5 miles from Augusta, Georgia, a metropolitan center of approximately 200,000 (US Census Bureau, [www.census.gov](http://www.census.gov)). Deciduous, broad leaf trees and shrubs compose  $\sim 80\%$  of the ground cover for much of the area surrounding the sampling site (Guenther et al., 2012, Figure S2). Samples for CO stable isotopes were collected approximately bi-monthly for one year (April 2015 – March 2016) from this site. This site uses “grab sampling” rather than the integrating sampling used at the INFLUX towers. Flasks are flushed and then filled

30

and pressurized over about a two minute period. Flasks are measured by the same methods as the INFLUX samples. However, although  $^{14}\text{CO}_2$  measurements are made on some flasks from this site, limitations on the available air in each flask mean that the CO stable isotopes were measured on different flasks (collected on different dates) than the  $^{14}\text{CO}_2$  measurements.

### 2.3 Stable Isotope Analysis

The stable isotopic measurement procedure is described in detail in Vimont et al. (2017). Briefly, the air is extracted from the PFP by vacuum transfer through a cold loop trap at  $-70^\circ\text{C}$  that removes water vapor. Next, a mass flow controller is used to regulate the flow of the sample through a second cryogenic trap at  $-196^\circ\text{C}$  that removes  $\text{CO}_2$ ,  $\text{N}_2\text{O}$ , and any other condensable species. The remaining air is passed through acidified  $\text{I}_2\text{O}_5$  suspended on a silica gel matrix (Schutze's reagent, (Schutze, 1944)) that quantitatively oxidizes CO to  $\text{CO}_2$ , adding an oxygen with a consistent isotopic signature. The sample passes through a second cold loop trap ( $-70^\circ\text{C}$ ) to remove any traces of sulfuric acid that has evolved from the reagent and finally the CO-derived  $\text{CO}_2$  is trapped on a third cryogenic trap ( $-196^\circ\text{C}$ ) while the remaining gasses are pumped away. The CO-derived  $\text{CO}_2$  is then transferred to a cryogenic focusing trap and finally released through a GC column (PoraBond Q) to the isotope ratio mass spectrometer (GV Instruments IsoPrime 5KeV).

Following convention, we use delta notation to report our isotopic results:

$$\delta^{13}\text{C}_{\text{VPDB}} = \left( \frac{R_s}{R_{\text{VPDB}}} - 1 \right) * 10^3\text{‰} \quad (1)$$

where  $R_s$  is the ratio of  $^{13}\text{C}$  to  $^{12}\text{C}$  in the sample and  $R_{\text{VPDB}}$  is the ratio of  $^{13}\text{C}$  to  $^{12}\text{C}$  in the international standard Vienna Pee Dee Belemnite. The same notation describes  $\delta^{18}\text{O}$  except the international standard of reference is Vienna Standard Mean Ocean Water (VSMOW). Because we are oxidizing CO to  $\text{CO}_2$  in this analysis, we correct our  $\text{CO}_2$   $\delta^{18}\text{O}$  data to account for the added oxygen, as described in Stevens and Krout (1972), Brenninkmeijer (1993), and Mak and Yang (1998):

$$\delta^{18}\text{O}_{\text{CO}} = 2\delta^{18}\text{O}_{\text{CO}_2} - (2\delta^{18}\text{O}_{\text{CO}_2\text{std}} - \delta^{18}\text{O}_{\text{COstd}}) \quad (2)$$

where the subscript CO indicates the original  $\delta^{18}\text{O}$  signature of the sample,  $\text{CO}_2$  indicates the  $\delta^{18}\text{O}$  of the  $\text{CO}_2$  measured in the mass spectrometer,  $\text{CO}_{2\text{std}}$  indicates the  $\delta^{18}\text{O}$  of the  $\text{CO}_2$  measured on the standard gas and  $\text{CO}_{\text{std}}$  indicates the calibrated  $\delta^{18}\text{O}$  of the CO in the same standard gas (standard gas procedure was described in Vimont et al. (2017)). Once the samples have been analyzed in the mass spectrometer, a correction for the  $^{17}\text{O}$  contribution to the  $\delta^{13}\text{C}$  measurement is applied to the data based on the recommendations of Brand et al. (2009) (Vimont et al., 2017). This correction is required because  $^{13}\text{C}$  and  $\text{C}^{17}\text{O}$  are indistinguishable in our mass spectrometer. The  $1\sigma$  repeatability over two years for our analysis system is 0.23‰ for  $\delta^{13}\text{C}$  and 0.46‰ for  $\delta^{18}\text{O}$ . For a more complete description of system performance, see Vimont et al. (2017).

We note that a significant deviation from the standard  $\text{CO}_2$   $^{17}\text{O}$  correction has been observed and quantified for CO (Röckmann and Brenninkmeijer, 1998; Röckmann et al., 1998). This so called “ $^{17}\text{O}$  excess”, or  $\Delta^{17}\text{O}$ , is a result of mass-independent fractionation (MIF) that arises in OH photolytic formation, which in turn affects CO during removal by OH (Röckmann et al., 1998b; Huff and Thiemens, 1998). Ozonolysis of VOC’s also contributes to  $^{17}\text{O}$  excess, (Röckmann et al., 1998 a,b). The source of CO from ozonolysis of VOC’s is discussed in more detail in section 3.4. The combined  $\Delta^{17}\text{O}$  from these processes can introduce error of up to 0.35‰ in the corrected  $\delta^{13}\text{C}$  values, and the error is only quantifiable by measuring  $\delta^{17}\text{O}$  (Röckmann and Brenninkmeijer, 1998b). However, though we do not measure  $\delta^{17}\text{O}$  for our samples, our data analysis approach (section 2.5) eliminates the need for this correction because both background and urban samples will see similar  $\Delta^{17}\text{O}$  effects. Additionally, because of the short transit time between our background and polluted tower sites (3.2 hours, section 2.1), and the long lifetime of most VOC ozonolysis relative to OH oxidation (Atkinson and Arey, 2003a), we expect any effect of ozonolysis produced  $\Delta^{17}\text{O}$  error to our  $\delta^{13}\text{C}$  measurements to be insignificant relative to our measurement uncertainty.

#### *2.4 Radiocarbon $\text{CO}_2$ Analysis*

30

Each of the INFLUX samples analyzed for the stable isotopes of CO was also analyzed for  $^{14}\text{CO}_2$ .  $^{14}\text{CO}_2$  is the best tracer for fossil fuel produced  $\text{CO}_2$  because fossil fuels contain no  $^{14}\text{C}$  (Levin et al., 2003; Turnbull et al., 2006).  $^{14}\text{CO}_2$  measurements were made by extracting  $\text{CO}_2$  from whole air in each flask at INSTAAR, University of Colorado, followed by graphitization and AMS  $^{14}\text{C}$  measurement at GNS Science, New Zealand (Turnbull et al., 2015b).  $\text{CO}_2\text{ff}$  was determined for each sample using Tower 1 as background, and the  $^{14}\text{CO}_2$  results for these and other INFLUX flask samples were reported in detail by Turnbull et al (2015) and Turnbull et al (2019).  $^{14}\text{C}$  measurements of  $\text{CO}_2$  are reported as  $\Delta^{14}\text{C}$ , or the permil deviation of the measured  $^{14}\text{C}$  from a standard material, corrected for fractionation effects and radioactive decay between sampling and measurement (Stuiver and Polach, 1977; Turnbull et al., 2015). The conversion of the  $^{14}\text{CO}_2$  measurements to  $\text{CO}_2\text{ff}$  enhancements is done by:

$$X_{\text{CO}_2\text{ffenh}} = \frac{X_{\text{CO}_2\text{obs}}(\Delta_{\text{obs}} - \Delta_{\text{bg}})}{(\Delta_{\text{ff}} - \Delta_{\text{bg}})} - \frac{X_{\text{CO}_2\text{other}}(\Delta_{\text{other}} - \Delta_{\text{bg}})}{(\Delta_{\text{ff}} - \Delta_{\text{bg}})} \quad (3)$$

(Turnbull et al., 2015).  $X_{\text{CO}_2\text{ffenh}}$  is calculated using the observed ( $\Delta_{\text{obs}}$ ) and background ( $\Delta_{\text{bg}}$ )  $\Delta^{14}\text{C}$  values and the observed  $\text{CO}_2$  mole fraction ( $X_{\text{CO}_2\text{obs}}$ ).  $\Delta_{\text{ff}}$  is the  $\Delta^{14}\text{C}$  value of fossil fuel  $\text{CO}_2$  (by definition -1000‰).  $X_{\text{CO}_2\text{other}}$  is a small correction that is applied and consists primarily of sources from the nuclear industry and heterotrophic respiration. Typical values for  $X_{\text{CO}_2\text{other}}$  are 0.2 - 0.5 ppm when a continental background is used (e.g. in Turnbull et al., 2006; Miller et al., 2012; Turnbull et al., 2015). The measurement precision of  $\sim 1.8\text{‰}$  results in uncertainties in  $\text{CO}_2\text{FF}$  of better than  $1 \mu\text{mol}:\text{mol} \text{CO}_2\text{FF}$  for these samples.

### 2.5 Regression Plot Analysis

At Indianapolis, the CO measured at tower 2 is typically 20 nmol:mol higher than the background CO of  $\sim 150$  nmol:mol at tower 1. It is necessary to remove the background signal from the polluted tower to accurately constrain the urban CO signals. Using the method described by Miller and Tans (2003), we calculate the isotopic signature of the urban source:

$$\delta_s = \frac{(\delta_{\text{meas}}X_{\text{CO}_{\text{meas}}} - \delta_{\text{bkg}}X_{\text{CO}_{\text{bkg}}})}{(X_{\text{CO}_{\text{meas}}} - X_{\text{CO}_{\text{bkg}}})} \quad (4)$$

where  $\delta_s$  is the  $\delta^{13}\text{C}$  or  $\delta^{18}\text{O}$  of the urban source (Figure 2), X indicates the mole fraction and the subscript “meas” indicates the  $\delta^{13}\text{C}$  (or  $\delta^{18}\text{O}$ ) and CO mole fraction measured at tower 2. The subscript “bkg” indicates the  $\delta^{13}\text{C}$  (or  $\delta^{18}\text{O}$ ) and CO mole fraction measured at tower 1.

5 In order to obtain a best-fit solution using (4) for all the data, we regressed the numerator against the denominator using an ordinary least squares (model 1) Y|X approach (Isobe et al., 1990; Zobitz et al., 2006).

To account for uncertainty in our measurements, we used a Monte Carlo technique. Using  
 10 the propagated measurement uncertainties, we assigned an error distribution to each point. We assumed a normally distributed error curve based on QQ plot analysis of our data against a synthetic normally distributed data set (not shown). This analysis allows us to assess if two data sets have the same distribution. 10,000 regressions were run, randomly selecting values for each data point from that point’s error distribution. The  
 15 reported slopes are the median values from the 10,000 regressions. The reported errors on the slope are  $1\sigma$  for the slopes of each simulation.

At the Beech Island measurement site, no local background measurement site with CO isotope measurements exists. Therefore, we performed a Keeling plot analysis, as well as a  
 20 Miller-Tans plot analysis using monthly averaged CO mole-fraction,  $\delta^{13}\text{C}$ , and  $\delta^{18}\text{O}$  data from Izaña, Tenerife in the Canary Islands (28°N, 16°W, 2370 masl) as a background for Beech Island (Bräunlich, 2000, Table S4). The Beech Island Miller Tans analysis was performed in the same manner as the Indianapolis source signatures, described above.

25 In the Keeling plot approach, isotopic measurements are plotted against the reciprocal of the mole fraction (Keeling, 1958). This method uses the relationship:

$$\delta_{\text{obs}} = \delta_s + M(X_{\text{CO}}^{-1}) \quad (5)$$

where  $\delta_{\text{obs}}$  is the observed  $\delta^{13}\text{C}$  or  $\delta^{18}\text{O}$  at the measurement site, M is the slope determined from a regression of the data, and  $X_{\text{CO}}$  is the observed CO mole fraction.  $\delta_s$  is the intercept

determined from a regression of the data. The intercept represents the isotopic signature of the sources influencing the measurement site (Keeling, 1958). The Keeling plot assumes that the background concentration and isotopic values are constant over the period of analysis, which is a reasonable but imperfect assumption for this dataset measured over the summer season. The benefits and limitations of this approach are discussed more fully in section 3.3.

To assess the uncertainty of our Keeling plot analysis, we perform a standard Monte Carlo analysis and additionally use a sampling with replacement Monte Carlo method (often referred to as a bootstrap Monte Carlo). Briefly, the bootstrap Monte Carlo consists of calculating a linear regression for 1000 randomly chosen sample sets. These sets are chosen from the original data, at random, such that the number of data points is always constant ( $n=7$  for both summer and winter at Beech Island). However, in some sample sets, points may be selected more than once, or not at all. In this way, any disproportionately large influence on the model by outlier points can be assessed, and the distribution of the model parameter of interest (in our case, the intercept) is representative of data as a whole. We report the mean of the 1000 intercepts, and both the  $1\sigma$  standard deviation as well as the standard error of the mean are reported for the error on that value. The bootstrap Monte Carlo distributions are shown in the supplementary material (section S3).

### *2.6 Calculation of the VOC oxidation isotopic signatures using mass balance*

The  $\text{CH}_4$  oxidation source, the biomass-burning source, and the OH oxidation sink have negligible impacts for the Indianapolis CO budget (detailed calculations can be found in the supplementary material, section S2). In order to constrain the remaining two sources (fossil fuel combustion and VOC oxidation), we use a simple isotope mass balance approach. We assume that the  $\delta_s$  calculated at each polluted tower (section 2.5, equation (4)) can be represented by:

$$\delta_s = f_{\text{VOC}}\delta_{\text{VOC}} + f_{\text{FF}}\delta_{\text{FF}} \quad (6a)$$

$$f_{\text{VOC}} = \frac{X_{\text{CO-VOC}}}{X_{\text{CO-ENH}}} \quad (6b)$$

$$f_{\text{FF}} = \frac{X_{\text{CO-FF}}}{X_{\text{CO-ENH}}} \quad (6c)$$

where  $f_{\text{VOC}}$  and  $\delta_{\text{VOC}}$  are the fraction (as compared to total urban CO enhancement) and isotopic signature of CO added from VOC oxidation, and  $f_{\text{FF}}$  and  $\delta_{\text{FF}}$  are the fraction and isotopic signature of CO added from fossil fuel combustion.  $X_{\text{CO-VOC}}$ ,  $X_{\text{CO-FF}}$ , and  $X_{\text{CO-ENH}}$  are the mole fractions for VOC-produced CO, the fossil fuel-produced CO, and the total urban CO enhancement, respectively. The isotopic signatures of fossil fuel combustion at Indianapolis were previously determined from wintertime measurements when fossil fuel combustion is the only significant CO source in Indianapolis and are  $-27.7 \pm 0.5\text{‰}$  and  $17.7 \pm 1.1\text{‰}$  for  $\delta^{13}\text{C}$  and  $\delta^{18}\text{O}$  respectively (Vimont et al., 2017). That study found that the isotopic signature in the winter did not vary significantly with temperature, and that the primary source within the city was emissions from transportation (Vimont et al., 2017). Therefore, we use these values as the fossil fuel produced CO isotopic signatures for Indianapolis. Because we have only two sources (supplementary material, section S2), we can derive  $X_{\text{CO-VOC}}$  as:

$$X_{\text{CO-VOC}} = X_{\text{CO-ENH}} - X_{\text{CO-FF}} \quad (7)$$

In order to determine  $X_{\text{CO-VOC}}$  we need to determine  $X_{\text{CO-FF}}$ . This is done using the fossil fuel CO to CO<sub>2</sub> ratio:

$$X_{\text{CO-FF}} = R_{\text{COFF:CO2FF}} * X_{\text{CO2-FF}} \quad (8)$$

where  $X_{\text{CO2-FF}}$  is the fossil fuel produced enhancement in the CO<sub>2</sub> mole fraction, determined by <sup>14</sup>CO<sub>2</sub> measurements (section 2.4).  $R_{\text{COFF:CO2FF}}$  is the ratio of CO<sub>FF</sub> to CO<sub>2FF</sub> and was determined to be  $7 \pm 1$  nmol:μmol for Indianapolis in the winter, when nearly all CO produced is from fossil fuel combustion, primarily vehicles (Turnbull et al., 2018). We assume that this ratio holds across all seasons. We then solve equations (8), (7) and (6a) to determine  $\delta_{\text{VOC}}$ . In order to estimate a mean value for our limited sample set, we perform a bootstrap Monte Carlo approach, similar to that described in the previous section. We perform 10,000 calculations of the mean. We report the mean and standard deviation of

the 10,000 individual mean values for our bootstrap Monte Carlo simulation as our estimate of the isotopic value and uncertainty of  $\delta_{\text{VOC}}$ .

5 Simple filtering is applied to these data. Any samples with calculated  $X_{\text{CO-VOC}}$  values that were near zero, negative, or exceeded the total urban enhancement were removed.  $X_{\text{CO-VOC}}$  values that are negative or exceed the total enhancement are obviously non-physical. Positive values of  $X_{\text{CO-VOC}}$  that are extremely low (less than 5% of the total enhancement), while physical, create extreme outliers when  $\delta^{13}\text{C}_{\text{VOC}}$  or  $\delta^{18}\text{O}_{\text{VOC}}$  are calculated (in one case, several hundred ‰). Likewise, cases where  $X_{\text{CO-VOC}}$  is calculated to be nearly the entire  
10 urban enhancement, our method will produce  $\delta_{\text{CO-VOC}}$  estimates which approach or are equal to our urban enhancement  $\delta$  values.

Large overestimates of  $X_{\text{CO-VOC}}$  arise because the ratio method can produce unrealistically low calculated  $X_{\text{CO-VOC}}$  values if the  $X_{\text{CO}_2\text{-FF}}$  enhancements are not significantly different from  
15 zero.  $X_{\text{CO}_2\text{-FF}}$  enhancements near or below zero are a result of possible local contamination at or near the background tower, which violates the assumption of well mixed background air flowing across the city. Conversely, the ratio method can overestimate  $X_{\text{CO-VOC}}$  thereby underestimate  $X_{\text{CO-VOC}}$  when  $X_{\text{CO}_2\text{-FF}}$  is highly elevated, without a corresponding elevation in  $X_{\text{CO-ENH}}$ . One example of how this can occur is if the local power plant (the Harding Street  
20 Power Plant) plume is sampled by the polluted tower. In the period of this study, the Harding Street Power Plant contributed about 28% of Indianapolis'  $\text{CO}_2\text{FF}$  emissions and, while this source is often dispersed, the plume from this source is occasionally observed at tower 2. This source has a  $\text{CO}:\text{CO}_2\text{FF}$  ratio of  $<0.1 \text{ nmol}:\mu\text{mol}$ , due to CO emissions controls fitted to the exhaust stack. Because we use a constant value for  $R_{\text{CO}:\text{CO}_2\text{FF}}$ , any day where  
25 tower 2 samples contain power plant emissions will produce low or negative  $X_{\text{CO-VOC}}$  values. We do not attempt to identify specific causes for high or low  $X_{\text{CO-VOC}}$  values. For our sample set, we simply filter samples in which  $X_{\text{CO-VOC}}$  was less than 15% of the total enhancement, which produced strong outliers, and samples in which  $X_{\text{CO-VOC}}$  was more than 85% of the total enhancement, which produced values equal to our calculated urban enhancements.

This filtering removed a total of 6 data points. The data used for calculating the isotopic signatures for VOC derived CO is shown in Table 2.

### 3. Results and Discussion

5

#### *3.1 Determination of the urban enhancement CO isotopic signatures*

The full time series from Indianapolis was published in Vimont et al. (2017). However, we have reproduced the data from towers 1 and 2 (Figure 3) here to highlight the summertime data (not discussed in Vimont et al., 2017). The summertime mole fraction and isotopic data can be seen in Table S2 in the supplementary material. One of the more salient features of the summer Indianapolis data as compared to the winter data is that, while tower 2 CO mole fraction remains enhanced over tower 1 throughout the year, the  $\delta^{18}\text{O}$  values at tower 2 tend to be much closer to those of tower 1 during the summer, yet are more positive during the winter. This is consistent with the hypothesis that the wintertime urban enhancement is dominated by a fossil source, while the summertime enhancement is a mixed source. Further, this mixed source must be more depleted in  $^{18}\text{O}$  than fossil fuel produced CO. The  $\delta^{13}\text{C}$  results are more difficult to interpret from the time series alone, which underscores the need for the Miller Tans method at Indianapolis.

20

The Miller Tans Monte Carlo regression analysis produced isotopic results of  $-29.6 \pm 1.0\text{‰}$  for  $\delta^{13}\text{C}$  and  $12.5 \pm 2.1\text{‰}$  for  $\delta^{18}\text{O}$  ( $1\sigma$ ) for the overall urban summertime CO source (Figure 2). The  $\delta^{13}\text{C}$  source signature is very similar to that determined in winter ( $-27.7 \pm 0.5\text{‰}$ , Vimont et al., 2017). In contrast, the  $\delta^{18}\text{O}$  signature is substantially lower in summer than in winter ( $17.7 \pm 1.0\text{‰}$  in winter, Vimont et al., 2017). These results are consistent with our hypothesized mixing of two sources of CO with different isotopic signatures contributing to the summertime CO enhancement. The determined  $\delta^{13}\text{C}$  of the urban CO source stays relatively consistent between winter and summer ( $-27.7 \pm 0.5\text{‰}$  and  $-29.6 \pm 1.0\text{‰}$ , respectively), suggesting that the VOC oxidation source must have a  $\delta^{13}\text{C}$  signature that is only slightly more negative than the fossil fuel source. In contrast,  $\delta^{18}\text{O}$  of

30

the urban source changes substantially from winter to summer ( $17.7 \pm 1.0\text{‰}$  and  $12.5 \pm 2.1\text{‰}$ , respectively), indicating a VOC  $\delta^{18}\text{O}$  signature that is much more negative than the fossil fuel source. The increased scatter in the  $\delta^{18}\text{O}$  regression relative to  $\delta^{13}\text{C}$  is also consistent with this interpretation: variability in the relative contributions of fossil fuel and VOC CO sources for different samples will impart more variability in  $\delta^{18}\text{O}$  than  $\delta^{13}\text{C}$ .

Day to day variability in the VOC oxidation source is expected and supports the hypothesis that secondary production of CO by VOCs strongly contributes to the urban enhancement. For example, isoprene has a short atmospheric lifetime in urban regions and rapidly forms CO (Atkinson and Arey, 2003). Isoprene oxidation is highly variable because isoprene emissions depend exponentially on the ambient temperature, and the rate at which isoprene is oxidized will increase as  $\text{NO}_x$  increases (Guenther et al., 1995; Carter and Atkinson, 1996). Additionally, boundary layer mixing will vary day to day, affecting the magnitude and transport of all sources within the tower domain.

15

### *3.2 Determination of the VOC-produced CO $\delta^{13}\text{C}$ and $\delta^{18}\text{O}$ isotope signature*

To determine the VOC-produced CO isotopic signature, we first determined the fossil fuel-produced  $\text{CO}_2$  source (section 2.4). The  $^{14}\text{CO}_2$ , the derived  $\text{CO}_{2\text{FF}}$  mole fractions, and the calculated  $\text{CO}_{\text{FF}}$  and  $\text{CO}_{\text{VOC}}$  mole fractions are presented in Table 2. The uncertainties reported are  $1\sigma$  for  $\text{CO}_{2\text{FF}}$  and  $\Delta^{14}\text{CO}_2$ , while the uncertainties on the calculated  $\text{CO}_{\text{FF}}$  and  $\text{CO}_{\text{VOC}}$  values are the propagated errors for equations (7) and (8). Using the mass balance approach and bootstrap Monte Carlo method described in section 2.6 we use the isotopic source signatures determined in section 3.1 to calculate the isotopic signatures of VOC-derived CO (Table 2) and the associated bootstrap Monte Carlo mean values:  $-32.8\text{‰} \pm 0.5\text{‰}$  for  $\delta^{13}\text{C}$  and  $3.6\text{‰} \pm 1.2\text{‰}$  for  $\delta^{18}\text{O}$  ( $1\sigma$ ). The scatter in the VOC-derived CO isotopic signatures calculated for individual samples is relatively large (Table 2), and likely due to a combination of uncertainties discussed in Section 2.6 and real day-to-day variability in the isotopic signatures. However, it is the mean values that are of most interest for CO budget studies, and these appear to be well constrained by the data set.

30

The  $\delta^{13}\text{C}$  results compare well to the later of previously published estimates of the VOC oxidation signature:  $-32 \pm 2 \text{‰}$  (e.g. Brenninkmeijer et al., 1999). This value is reasonable given the expected carbon isotopic ratio of isoprene and the fractionation processes associated with the isoprene oxidation reaction (e.g. Sharkey et al., 1991). Our  $\delta^{18}\text{O}$  result compares well with the previously published estimate from Brenninkmeijer and Röckmann (1997) ( $\sim 0\text{‰}$ ) but contradicts Stevens and Wagner (1989) ( $\sim 15\text{‰}$ ). We re-examine the methods and uncertainties of the previous studies to understand what might cause this discrepancy.

10

Stevens and Wagner (1989) performed a Keeling plot analysis of samples collected in rural Illinois. They assumed a constant background, with VOC oxidation as the only added CO source, and performed a Keeling plot analysis. Their results indicated  $-32.2\text{‰}$  for  $\delta^{13}\text{C}$  and  $15\text{‰}$  for  $\delta^{18}\text{O}$  of the added CO source. They also measured four samples from a coastal site in Australia and obtained an average  $\delta^{18}\text{O}$  of  $5\text{‰}$  for the atmospheric  $\text{C}^{18}\text{O}$  signature. They did not perform a Keeling analysis on the Australian data. They reasoned that the effect of oxidation by OH on the Australia samples would reduce the  $\delta^{18}\text{O}$  by  $10\text{‰}$ , which meant the source (assumed to be dominated by VOC and methane oxidation) must have been  $15\text{‰}$ , in agreement with their rural Illinois samples.

20

The value of  $0\text{‰}$  suggested by Brenninkmeijer and Röckmann (1997) was based on a model-driven interpretation of CO isotope measurements in the southern hemisphere. Using mass balance, they were able to determine the oxidation of methane and VOCs should produce CO with an oxygen isotopic value near to  $0\text{‰}$ , while the value of  $15\text{‰}$  suggested by Stevens and Wagner (1989) could not be consistent with the measurements. Bergamaschi et al. (2000) used an atmospheric inversion combined with CO mole fraction and isotopic measurements in an attempt to determine the isotopic signatures of CO sources at the global scale. However, their study resulted in wide ranges for  $\delta^{13}\text{C}$  ( $-17\text{‰}$  to  $-31\text{‰}$ ) and  $\delta^{18}\text{O}$  ( $-30\text{‰}$  to  $+23\text{‰}$ ) isotopic values, dependent on the input parameters of their model. Later studies using  $\delta^{18}\text{O}$  to partition the global budget generally use the  $0\text{‰}$

30

value for  $\delta^{18}\text{O}$  despite the lack of consensus (e.g., Park et al., 2015). By leveraging the INFLUX measurements, we are able to place a constraint on the VOC-produced CO isotopic signatures without relying on the uncertain assumptions of a constant background / VOCs as the only source, or on the use of a model to derive the CO mass balance.

5

### *3.3 Beech Island South Carolina Isotopic Data*

The Beech Island results are shown in Figure 4, while the data can be found in the supplementary information (Table S3). One of the most striking features of this data set is that while the  $\delta^{13}\text{C}$  and  $\delta^{18}\text{O}$  both decrease from spring into summer and then increase into the fall and winter, the mole fraction values do not exhibit much seasonality. While any true seasonal cycles or trends are impossible to determine with only a single year of data, this nonetheless is consistent with a strong summer source of CO from VOC oxidation.

15 The Keeling plot-derived CO source isotopic signatures at Beech Island, South Carolina are shown in Figure 5. During the summer months (June-July-August-September), the Keeling plot analysis (section 2.5) produces a  $\delta^{13}\text{C}$  signature of  $-31.2\text{‰} \pm 0.2\text{‰}$  and a  $\delta^{18}\text{O}$  signature of  $5.8\text{‰} \pm 0.7\text{‰}$  ( $1\sigma$ ) using a standard Monte Carlo simulation and a  $\delta^{13}\text{C}$  signature of  $-30.9\text{‰} \pm 5.7\text{‰}$ , and a  $\delta^{18}\text{O}$  signature of  $5.6\text{‰} \pm 2.4\text{‰}$  ( $1\sigma$ ) using the bootstrap Monte Carlo method. During the winter months (December-January-February-March), we obtain a  $\delta^{13}\text{C}$  signature of  $-27.3\text{‰} \pm 0.2\text{‰}$  and a  $\delta^{18}\text{O}$  signature of  $21.1\text{‰} \pm 0.3\text{‰}$  ( $1\sigma$ ) using the standard Monte Carlo method. Using the bootstrap Monte Carlo, we obtain a  $\delta^{13}\text{C}$  of  $-26.8\text{‰} \pm 3.7\text{‰}$  and a  $\delta^{18}\text{O}$  of  $20.4\text{‰} \pm 5.0\text{‰}$  ( $1\sigma$ ). The Keeling approach implicitly assumes constant background CO mole fraction and isotopic composition, which is unlikely to be correct for Beech Island for the entire duration of the summer. However, this approach is still useful for an approximate estimation of the CO source isotopic composition. This is particularly true for  $\delta^{18}\text{O}$ , where the difference between the inferred source isotopic signature and the measured  $\delta^{18}\text{O}$  values is larger than the scatter in the measured values.

30

In an alternative approach, we apply a background seasonal signal from data published by Bräunlich (2000) from Izaña, Tenerife to allow for a Miller-Tans plot analysis. Tenerife is located in a similar latitudinal band to Beech Island (28°N vs 33.4°N), and the amplitude of the background seasonal signal should be similar between the two sites. However, the  
5 Tenerife data set is from sampling done approximately two decades before our Beech Island sampling, and therefore global changes to the CO budget between the two studies will introduce error to this analysis that is not easily quantified. Figure 6 shows the isotopic source signatures derived from a Monte Carlo simulation for a Miller Tans plot approach using monthly averaged data from Izaña, Tenerife (Bräunlich, 2000) as a  
10 background for Beech Island. This method produced summer (June-July-August-September)  $\delta^{13}\text{C}$  and  $\delta^{18}\text{O}$  source signatures of  $-29.5\text{‰} \pm 3.2\text{‰}$  and  $5.8\text{‰} \pm 0.3\text{‰}$  ( $1\sigma$ ) respectively. During the winter months (December, January, February, March), we obtained  $\delta^{13}\text{C}$  and  $\delta^{18}\text{O}$  source signatures of  $-27.2\text{‰} \pm 3.7\text{‰}$  and  $20.5\text{‰} \pm 1.7\text{‰}$  ( $1\sigma$ ), respectively. These results are in good agreement with our Keeling plot results.

15 While both the Keeling and the Miller-Tans approaches for analyzing Beech Island data have important weaknesses as discussed above, these weaknesses are different. The close agreement between the Keeling and Miller Tans approaches for Beech Island therefore increases confidence in our findings and suggests that the primary drivers of the observed  
20 isotopic source signatures are local sources, rather than seasonal changes in background CO. The mean values (and standard deviations) of the isotopic signatures at Beech Island from our three analyses are  $-30.5\text{‰} \pm 3.2\text{‰}$  and  $5.7\text{‰} \pm 0.8\text{‰}$  during the summer, and  $-27.1\text{‰} \pm 3.7\text{‰}$  and  $20.7\text{‰} \pm 1.7\text{‰}$  during the winter for  $\delta^{13}\text{C}$  and  $\delta^{18}\text{O}$  respectively.

25 The wintertime source signatures derived at Beech Island are consistent with prior estimates of fossil fuel combustion sources ( $\delta^{13}\text{C}$ :  $\sim -27.5\text{‰}$ ,  $\delta^{18}\text{O}$ :  $\sim 23.5\text{‰}$ , Table 1). The Beech Island  $\delta^{13}\text{C}$  value is consistent with the wintertime value found at Indianapolis ( $-27.7\text{‰} \pm 0.5\text{‰}$ , Vimont et al., 2017), while the  $\delta^{18}\text{O}$  value differs slightly from the value found at Indianapolis during the winter ( $17.7\text{‰} \pm 1\text{‰}$ , Vimont et al., 2017). At  
30 Indianapolis, the winter CO urban enhancement was found to be primarily fossil fuel in origin, but it was noted that the oxygen isotopic signature was significantly different from

prior estimates of fossil fuel combustion, possibly due to Indianapolis' emission regulation (Vimont et al., 2017). Nonetheless, this suggests that the main driver of CO variability during the winter at Beech Island is likewise fossil fuel combustion. In contrast, the summer CO source isotopic signatures at Beech Island ( $\delta^{13}\text{C}$ : -30.5‰,  $\delta^{18}\text{O}$ : 5.7‰) are lower than for Indianapolis ( $\delta^{13}\text{C}$ : -29.6‰,  $\delta^{18}\text{O}$ : 12.5‰), which is consistent with a larger relative contribution of CO from VOC oxidation. As stated above, the absence of a clear CO mole fraction summertime minimum at Beech Island (Figure 4) is likely due to the large influence from CO produced by oxidation of VOCs during the summer, which offsets the expected summertime CO decline, such as is seen at Indianapolis (Figure 3). The much higher contribution of CO produced by oxidized VOCs at Beech Island relative to Indianapolis is reasonable, given the more concentrated fossil fuel source in the Indianapolis urban area and the higher concentrations of biogenic VOCs expected at the densely forested and warmer Beech Island site.

While the small dataset from Beech Island does not allow for a direct estimate of the isotopic signatures of VOC-produced CO, it is consistent with the values we obtained from Indianapolis and with values estimated by Brenninkmeijer and Röckmann (1997). Additionally, the Beech Island data is not consistent with the 15‰ value for  $\delta^{18}\text{O}$  of VOC-produced CO suggested by the prior Stevens and Wagner (1989) study. The Beech Island data suggest the dominant local CO wintertime source is fossil fuel combustion, with a  $\delta^{18}\text{O}$  isotopic signature of approximately 20‰. During the summer months, the addition of VOC-produced CO shifts the overall source  $\delta^{18}\text{O}$  to approximately 6‰. If the oxygen isotopic signature of CO produced by oxidation of VOCs was 15‰, as suggested by Stevens and Wagner (1989), this result would be impossible.

25

### *3.4 Discussion of the role of ozonolysis in the VOC-derived CO $\delta^{18}\text{O}$ signature*

As noted above, Röckmann et al. (1998) suggested ozonolysis of VOC's may be a cause of significant  $\Delta^{17}\text{O}$  deviations resulting from mass independent fractionation (MIF) during the formation of  $\text{O}_3$  (see Röckmann et al. (1998a,b) for a more detailed explanation of the MIF process). Hatakeyama et al. (1991), Röckmann et al. (1998a), and Atkinson and Arey

30

(2003 a,b) have suggested that ozonolysis may be a large sink for terpenes in the atmosphere.

Röckmann et al., (1998a) found that  $O_3$ , and subsequently the CO produced from ozonolysis of VOC's, had a substantially enriched  $\delta^{18}O$  signature relative to atmospheric oxygen and CO. The  $\delta^{18}O$  of  $O_3$  was shown to be around 80‰, and ethene, isoprene, and  $\beta$ -pinene produced CO with a  $\delta^{18}O$  between 46‰ and 83‰ (relative to the original  $O_2$  used in the experiments) (Röckmann et al., 1998a). The  $\delta^{18}O$  of atmospheric  $O_2$  is around 23‰, and therefore the CO produced by ozonolysis of these VOC's in the atmosphere would have a  $\delta^{18}O$  of between 69‰ to 100‰. Röckmann et al. (1998a) acknowledge that a significant global source of CO with a  $\delta^{18}O$  of 69‰-100‰ is difficult to reconcile with the overall CO  $\delta^{18}O$  budget, and thus conclude that either a) ozonolysis of VOC's is not the primary source of the observed mass independent  $^{17}O$  deviations, or b) a second source with sufficiently depleted  $\delta^{18}O$  and similar seasonal cycle to ozone, VOC emissions, and CO must be countering the ozonolysis  $\delta^{18}O$  contribution. Röckmann et al. (1998b) detail a second source of MIF from CO+OH, and concluded that the ozonolysis source was a small contributor to the overall CO budget.

Our  $\delta^{18}O$  time series (Figures 3 and 4) as well as summertime source isotopic signature analyses (Figures 2, 5, 6) are not consistent with a summertime source with such a strong enrichment in  $^{18}O$ . Röckmann et al. (1998a) found no evidence for a seasonally covarying source that has depleted  $^{18}O$  of a similar magnitude to the ozonolysis source, that could obscure the impact of ozonolysis on CO- $\delta^{18}O$ . Thus, we conclude that CO produced by the ozonolysis of VOCs is not a major component of the CO budget at both Indianapolis and Beech Island, and that OH oxidation is the dominant source of VOC produced CO in our study.

Nonetheless, our  $\delta^{18}O$  results do not preclude a minor source of CO from ozonolysis of VOCs and the VOC produced CO  $\delta^{13}C$  and  $\delta^{18}O$  signatures calculated in this study cannot be separated between OH oxidation and ozonolysis. We note that, as discussed in section 2.1, the mean transit time for air masses between our background and polluted sites is 3.2

hours, which favors the oxidation of isoprene by OH (lifetime  $\sim 1.4$  hours) relative to ozonolysis (lifetime  $\sim 1.3$  day), depending on the OH and O<sub>3</sub> concentrations (Atkinson and Arey, 2003a).  $\beta$ -pinene (also tested by Röckmann et al. (1998a)) has similar OH and O<sub>3</sub> lifetimes (1.8 hours vs 1.1 days, respectively) (Atkinson and Arey, 2003a). Furthermore, 5 Atkinson (2000) and Atkinson and Arey (2003a,b) have detailed the reaction schemes for VOCs, and the OH oxidation and ozonolysis pathways, which are complex. Ozonolysis of isoprene, for example, produces an ozonide which is then destroyed via three possible reaction pathways (Atkinson, 2000; Atkinson and Arey, 2003a,b). Only one of these 10 pathways produces formaldehyde, which is subsequently photolyzed and the only pathway by which the oxygen isotopic signature of ozone could be guaranteed to be preserved in the resultant CO (Atkinson, 2000; Atkinson and Arey, 2003a,b). Other reaction pathways involve further interaction with OH or other molecules (Atkinson, 2000; Atkinson and Arey, 2003a,b), which provides for possible fractionation or exchange of the oxygen isotopes. Other terpenes also form higher order aldehydes, which primarily react with OH or NO<sub>3</sub>, 15 but do not react further with O<sub>3</sub> (Atkinson, 2000; Atkinson and Arey, 2003a,b). For reaction pathways other than photolysis of formaldehyde, the oxygen isotope fractionations or exchanges are difficult to trace and quantify, and are beyond the scope of this study.

20 To conclude, our results for the  $\delta^{13}\text{C}$  and  $\delta^{18}\text{O}$  signature of CO produced by oxidation of VOC's mainly represent OH oxidation processes with possible minor contributions from ozonolysis. Our atmospheric  $\delta^{18}\text{O}$  timeseries from Indianapolis and Beech Island are consistent with prior CO isotopic studies, for example Mak et al. (2003) and Röckmann et al. (2002): they do not show evidence for a strong source of CO from ozonolysis of VOCs.

25

#### 4. Conclusions

We analyzed carbon monoxide stable isotopes and  $\Delta^{14}\text{CO}_2$  during three summers at Indianapolis and determined the isotopic signature of the urban CO enhancement during 30 the summer. Additionally, we analyzed CO stable isotopes approximately bi-monthly for one year at Beech Island, South Carolina. Using the  $\Delta^{14}\text{CO}_2$  data and the ratio of CO:CO<sub>2FF</sub>,

we calculated the fossil fuel component of the CO mole fraction enhancement at Indianapolis. We then used isotope mass balance and the Indianapolis CO<sub>FF</sub> isotopic signatures from prior work to calculate the isotopic signature of CO produced from VOCs: - 32.8‰ ± 0.5‰ for δ<sup>13</sup>C and 3.6‰ ± 1.2‰ for δ<sup>18</sup>O. This result mainly reflects oxidation  
5 of VOC's by OH, with a possible minor contribution from ozonolysis of VOC's. Our measurements from Beech Island, SC (a forest site strongly influenced by VOC-derived CO) are consistent with these results, and confirm that VOC-derived CO is a large component of the summer Beech Island CO budget. Our estimate for the carbon isotopic signature of VOC-produced CO agrees well with and confirms prior estimates. Our oxygen isotopic  
10 result agrees well with estimates made by Brenninkmeijer and Röckmann (1997) but does not support prior work by Stevens and Wagner (1989).

This result is an important step to improving the constraints on global and regional CO budgets. Additional studies that quantify the isotopic signature of VOC-produced CO could  
15 confirm whether our result is valid regionally and globally, as well as attempt to better quantify the global importance of CO produced via ozonolysis of VOCs.

*Author contributions:*

20 IJV performed the measurements, data analysis, and wrote the article. JCT assisted in data analysis and provided multiple coauthor revisions. VVP provided assistance with measurement issues, data analysis, and multiple coauthor revisions. PFP assisted in several of the measurements. CS provided several coauthor revisions. NM and SR provided logistical support for sample collection for the measurements. BHV and JWCW provided  
25 laboratory and equipment support.

*Competing Financial Interests:*

There are no competing financial interests for any of the authors.

30 *Funding Sources:*

This research was generously funded by the National Institute of Standards and Technology (grant 60NANB10D023) and the National Oceanic and Atmospheric Administration Climate Program Office's AC4 program (award NA13OAR4310074). The lead author and the analysis system development were supported through funding in  
5 conjunction with the INSTAAR contract for isotopic analysis (RA-133R-15-CQ-0044) with The National Oceanic and Atmospheric Administration (NOAA) Earth System Research Laboratory (ESRL) Global Monitoring Division (GMD) Global Greenhouse Gas Reference Network (GGGRN).

10 *Materials and Correspondence:*

Please direct all requests for materials and correspondence to Isaac J Vimont,  
[Isaac.vimont@colorado.edu](mailto:Isaac.vimont@colorado.edu)

*Data Availability:*

15 Data for this experiment is available in Table 2 in the manuscript, and the supplemental material.

## References

- Atkinson, R., and Arey, J.: Gas-phase tropospheric chemistry of biogenic volatile organic compounds: a review, *Atmospheric Environment*, 37, Supplement 2, 197-219, [http://dx.doi.org/10.1016/S1352-2310\(03\)00391-1](http://dx.doi.org/10.1016/S1352-2310(03)00391-1), 2003a.
- Atkinson, R., and Arey, J.: Atmospheric degradation of volatile organic compounds, *Chem. Rev.*, 103, 4605-4638, 10.1021/cr0206420, 2003b.
- Bergamaschi, P., Brenninkmeijer, C. A. M., Hahn, M., Röckmann, T., Scharffe, D. H., Crutzen, P. J., Elansky, N. F., Belikov, I. B., Trivett, N. B. A., and Worthy, D. E. J.: Isotope analysis based source identification for atmospheric CH<sub>4</sub> and CO sampled across Russia using the Trans-Siberian railroad, *J. Geophys. Res.-Atmos.*, 103, 8227-8235, 10.1029/97jd03738, 1998.
- Bergamaschi, P., Hein, Ralf, Brenninkmeijer, Carl A.M., Crutzen, Paul J.: Inverse modeling of the global CO cycle 2. Inversion of <sup>13</sup>C/<sup>12</sup>C and <sup>18</sup>O/<sup>16</sup>O isotope ratios, *Journal of Geophysical Research*, 105, 1929-1945, 2000.
- Brand, W. A., Assonov, S. S., and Coplen, T. B.: Correction for the <sup>17</sup>O Interference in δ<sup>13</sup>C Measurements When Analyzing CO<sub>2</sub> with Stable Isotope Mass Spectrometry, International Union of Pure and Applied Chemistry Inorganic Chemistry Division Commission on Isotopic Abundances and Atomic Weights, 2009.
- Bräunlich, M.: Study of atmospheric carbon monoxide and methane using isotopic analysis, PhD, Institute of Environmental Physics, Rupertus Carola University, Heidelberg, Germany, 2000.
- Brenninkmeijer, C. A. M.: Measurement of the Abundance of <sup>14</sup>CO in the Atmosphere and the <sup>13</sup>C/<sup>12</sup>C and <sup>18</sup>O/<sup>16</sup>O Ratio of Atmospheric CO with Applications in New Zealand and Antarctica, *Journal of Geophysical Research*, 98, 10,595-510,614, 1993.
- Brenninkmeijer, C. A. M., and Röckmann, T.: Principal factors determining the <sup>18</sup>O/<sup>16</sup>O ratio of atmospheric CO as derived from observations in the southern hemispheric troposphere and lowermost stratosphere, *Journal of Geophysical Research*, 102, 25477, 10.1029/97jd02291, 1997.
- Brenninkmeijer, C. A. M., Röckmann, T., Bräunlich, M., Jockel, P., and Bergamaschi, P.: Review of Progress in Isotope Studies of Atmospheric Carbon Monoxide, *Chemosphere- Global Change Science*, 1, 33-52, 1999.
- Carter, W. P. L., and Atkinson, R.: Development and evaluation of a detailed mechanism for the atmospheric reactions of isoprene and NO<sub>x</sub>, *Int. J. Chem. Kinet.*, 28, 497-530, 10.1002/(sici)1097-4601(1996)28:7<497::aid-kin4>3.0.co;2-q, 1996.

- Chameides, W. L., Lindsay, R. W., Richardson, J., and Kiang, C. S.: The role of biogenic hydrocarbons in urban photochemical smog - Atlanta as a case study, *Science*, 241, 1473-1475, 10.1126/science.3420404, 1988.
- Cheng, Y., Wang, Y. H., Zhang, Y. Z., Chen, G., Crawford, J. H., Kleb, M. M., Diskin, G. S., and Weinheimer, A. J.: Large biogenic contribution to boundary layer O<sub>3</sub>-CO regression slope in summer, *Geophysical Research Letters*, 44, 7061-7068, 10.1002/2017gl074405, 2017.
- Conny, J. M., and Currie, L. A.: The isotopic characterization of methane, non-methane hydrocarbons and formaldehyde in the troposphere, *Atmospheric Environment*, 30, 621-638, 10.1016/1352-2310(95)00305-3, 1996.
- Conny, J. M., Verkouteren, R. M., and Currie, L. A.: Carbon 13 composition of tropospheric CO in Brazil: A model scenario during the biomass burn season, *J. Geophys. Res.-Atmos.*, 102, 10683-10693, 10.1029/97jd00407, 1997.
- Daniel, J. S., and Solomon, S.: On the climate forcing of carbon monoxide, *J. Geophys. Res.-Atmos.*, 103, 13249-13260, 10.1029/98jd00822, 1998.
- Duncan, B. N., Logan, J. A., Bey, I., Megretskaia, I. A., Yantosca, R. M., Novelli, P. C., Jones, N. B., and Rinsland, C. P.: Global budget of CO, 1988–1997: Source estimates and validation with a global model, *Journal of Geophysical Research: Atmospheres*, 112, D22301, 10.1029/2007jd008459, 2007.
- Granier, C., Bessagnet, B., Bond, T., D'Angiola, A., van der Gon, H. D., Frost, G. J., Heil, A., Kaiser, J. W., Kinne, S., Klimont, Z., Kloster, S., Lamarque, J. F., Liousse, C., Masui, T., Meleux, F., Mieville, A., Ohara, T., Raut, J. C., Riahi, K., Schultz, M. G., Smith, S. J., Thompson, A., van Aardenne, J., van der Werf, G. R., and van Vuuren, D. P.: Evolution of anthropogenic and biomass burning emissions of air pollutants at global and regional scales during the 1980-2010 period, *Clim. Change*, 109, 163-190, 10.1007/s10584-011-0154-1, 2011.
- Griffin, R. J., Chen, J. J., Carmody, K., Vutukuru, S., and Dabdub, D.: Contribution of gas phase oxidation of volatile organic compounds to atmospheric carbon monoxide levels in two areas of the United States, *J. Geophys. Res.-Atmos.*, 112, 19, 10.1029/2006jd007602, 2007.
- Gros, V., Braunlich, M., Röckmann, T., Jockel, P., Bergamaschi, P., Brenninkmeijer, C. A. M., Rom, W., Kutschera, W., Kaiser, A., Scheel, H. E., Mandl, M., van der Plicht, J., and Possnert, G.: Detailed analysis of the isotopic composition of CO and characterization of the air masses arriving at Mount Sonnblick (Austrian Alps), *Journal of Geophysical Research*, 106, 3179-3193, 2001.
- Guenther, A., Hewitt, C. N., Erickson, D., Fall, R., Geron, C., Graedel, T., Harley, P., Klinger, L., Lerdau, M., McKay, W. A., Pierce, T., Scholes, B., Steinbrecher, R., Tallamraju, R.,

- Taylor, J., and Zimmerman, P.: A global model of natural volatile organic compound emissions, *J. Geophys. Res.-Atmos.*, 100, 8873-8892, 10.1029/94jd02950, 1995.
- Guenther, A. B., Jiang, X., Heald, C. L., Sakulyanontvittaya, T., Duhl, T., Emmons, L. K., and Wang, X.: The Model of Emissions of Gases and Aerosols from Nature version 2.1 (MEGAN2.1): an extended and updated framework for modeling biogenic emissions, *Geosci. Model Dev.*, 5, 1471-1492, 10.5194/gmd-5-1471-2012, 2012.
- Guenther, A. B., Zimmerman, P. R., Harley, P. C., Monson, R. K., and Fall, R.: Isoprene and monoterpene emission rate variability - model evaluations and sensitivity analyses, *J. Geophys. Res.-Atmos.*, 98, 12609-12617, 10.1029/93jd00527, 1993.
- Harley, C. P., Monson, K. R., and Lerdau, T. M.: Ecological and evolutionary aspects of isoprene emission from plants, *Oecologia*, 118, 109-123, 10.1007/s004420050709, 1999.
- Hatakeyama, S., Izumi, K., Fukuyama, T., Akimoto, H., and Washida, N.: Reactions of OH with alpha-pinene and beta-pinene in air- estimate of global CO production from the atmospheric oxidation of terpenes, *J. Geophys. Res.-Atmos.*, 96, 947-958, 10.1029/90jd02341, 1991.
- Helmig, D., Greenberg, J., Guenther, A., Zimmerman, P., and Geron, C.: Volatile organic compounds and isoprene oxidation products at a temperate deciduous forest site, *J. Geophys. Res.-Atmos.*, 103, 22397-22414, 10.1029/98jd00969, 1998.
- Holloway, T., Levy, H., and Kasibhatla, P.: Global distribution of carbon monoxide, *J. Geophys. Res.-Atmos.*, 105, 12123-12147, 10.1029/1999jd901173, 2000.
- Huff, A. K., and Thiemens, M. H.: O-17/O-16 and O-18/O-16 isotope measurements of atmospheric carbon monoxide and its sources, *Geophysical Research Letters*, 25, 3509-3512, 10.1029/98gl02603, 1998.
- Isobe, T., Feigelson, E. D., Akritas, M. G., and Babu, G. J.: Linear Regression in Astronomy, *Astrophys. J.*, 364, 104-113, 10.1086/169390, 1990.
- Kanakidou, M., and Crutzen, P. J.: The photochemical source of carbon monoxide: Importance, uncertainties and feedbacks, *Chemosphere - Global Change Science*, 1, 91-109, 1999.
- Keeling, C. D.: The concentration and isotopic abundances of atmospheric carbon dioxide in rural areas, *Geochimica Et Cosmochimica Acta*, 13, 322-334, 10.1016/0016-7037(58)90033-4, 1958.
- Levin, I., Kromer, B., Schmidt, M., and Sartorius, H.: A novel approach for independent budgeting of fossil fuel CO<sub>2</sub> over Europe by <sup>14</sup>C observations, *Geophysical Research Letters*, 30, 10.1029/2003gl018477, 2003.

- Logan, J. A., Prather, M. J., Wofsy, S. C., and McElroy, M. B.: Tropospheric Chemistry: A Global Perspective, *Journal of Geophysical Research*, 86, 7210-7254, 1981.
- Mak, J. E., and Kra, G.: The isotopic composition of carbon monoxide at Montauk Point, Long Island, *Chemosphere- Global Change Science*, 1, 205-218, 1999.
- Mak, J. E., Kra, G., Sandomenico, T., and Bergamaschi, P.: The seasonally varying isotopic composition of the sources of carbon monoxide at Barbados, West Indies, *J. Geophys. Res.-Atmos.*, 108, 10.1029/2003jd003419, 2003.
- Mak, J. E., and Yang, W.: Technique for Analysis of Air Samples for  $^{13}\text{C}$  and  $^{18}\text{O}$  in Carbon Monoxide via Continuous-Flow Isotope Ratio Mass Spectrometry, *Analytical Chemistry*, 70, 5159-5161, 1998.
- Manning, M. R., Brenninkmeijer, C. A. M., and Allan, W.: Atmospheric carbon monoxide budget of the southern hemisphere: Implications of  $^{13}\text{C}/^{12}\text{C}$  measurements, *Journal of Geophysical Research*, 102, 10673, 10.1029/96jd02743, 1997.
- Miles, N. L., Richardson, S. J., Lauvaux, T., Davis, K. J., Balashov, N. V., Deng, A., Turnbull, J. C., Sweeney, C., Gurney, K. R., Patarasuk, R., Razlivanov, I., Cambaliza, M. O. L., and Shepson, P. B.: Quantification of urban atmospheric boundary layer greenhouse gas dry mole fraction enhancements in the dormant season: Results from the Indianapolis Flux Experiment (INFLUX), *Elem Sci Anth*, 5, <http://doi.org/10.1525/elementa.127>, 2017.
- Miller, J. B., Lehman, S. J., Montzka, S. A., Sweeney, C., Miller, B. R., Karion, A., Wolak, C., Dlugokencky, E. J., Southon, J., Turnbull, J. C., and Tans, P. P.: Linking emissions of fossil fuel  $\text{CO}_2$  and other anthropogenic trace gases using atmospheric ( $\text{CO}_2$ )- $\text{C}-14$ , *J. Geophys. Res.-Atmos.*, 117, 23, 10.1029/2011jd017048, 2012.
- Miller, J. B., and Tans, P. P.: Calculating isotopic fractionation from atmospheric measurements at various scales, *Tellus Ser. B-Chem. Phys. Meteorol.*, 55, 207-214, 10.1034/j.1600-0889.2003.00020.x, 2003.
- Park, K., Emmons, L. K., Wang, Z. H., and Mak, J. E.: Joint Application of Concentration and  $\delta^{18}\text{O}$  to Investigate the Global Atmospheric  $\text{CO}$  Budget, *Atmosphere*, 6, 547-578, 10.3390/atmos6050547, 2015.
- Popa, M. E., Vollmer, M. K., Jordan, A., Brand, W. A., Pathirana, S. L., Rothe, M., and Röckmann, T.: Vehicle emissions of greenhouse gases and related tracers from a tunnel study:  $\text{CO}:\text{CO}_2$ ,  $\text{N}_2\text{O}:\text{CO}_2$ ,  $\text{CH}_4:\text{CO}_2$ ,  $\text{O}-2:\text{CO}_2$  ratios, and the stable isotopes  $\text{C}-13$  and  $\text{O}-18$  in  $\text{CO}_2$  and  $\text{CO}$ , *Atmospheric Chemistry and Physics*, 14, 2105-2123, 10.5194/acp-14-2105-2014, 2014.

- Röckmann, T., and Brenninkmeijer, C. A. M.: The error in conventionally reported  $^{13}\text{C}/^{12}\text{C}$  ratios of atmospheric CO due to the presence of mass independent oxygen isotope enrichment, *Geophysical Research Letters*, 25, 3163-3166, 1998.
- Röckmann, T., Brenninkmeijer, C. A. M., Neeb, P., and Crutzen, P. J.: Ozonolysis of nonmethane hydrocarbons as a source of the observed mass independent oxygen isotope enrichment in tropospheric CO, *J. Geophys. Res.-Atmos.*, 103, 1463-1470, 10.1029/97jd02929, 1998a.
- Röckmann, T., Brenninkmeijer, C. A. M., Saueressig, G., Bergamaschi, P., Crowley, J. N., Fischer, H., and Crutzen, P. J.: Mass-Independent Oxygen Isotope Fractionation in Atmospheric CO as a Result of the Reaction  $\text{CO}+\text{OH}$ , *Science*, 281, 544-546, 10.1126/science.281.5376.544, 1998b.
- Röckmann, T., Jockel, P., Gros, V., Bräunlich, M., Possnert, G., and Brenninkmeijer, C. A. M.: Using  $^{14}\text{C}$ ,  $^{13}\text{C}$ ,  $^{18}\text{O}$ , and  $^{17}\text{O}$  isotopic variations to provide insights into the high northern latitude surface CO inventory, *Atmospheric Chemistry and Physics*, 2, 147-159, 2002.
- Saurer, M., Prevot, A. S. H., Dommen, J., Sandradewi, J., Baltensperger, U., and Siegwolf, R. T. W.: The influence of traffic and wood combustion on the stable isotopic composition of carbon monoxide, *Atmospheric Chemistry and Physics*, 9, 3147-3161, 2009.
- Schutze, M.: New Oxidation Means for the Quantitative Crossover from carboxide to carbon dioxide- Article on the chemistry of iodine pentoxide, *Berichte der Deutschen Chemischen Gesellschaft*, 77, 484-487, 1944.
- Sharkey, T. D., Loreto, F., Delwiche, C. F., and Treichel, I. W.: Fractionation of carbon isotopes during biogenesis of atmospheric isoprene *Plant Physiol.*, 97, 463-466, 10.1104/pp.97.1.463, 1991.
- Stevens, C. M., Kaplan, L., Gorse, R., Durkee, S., Compton, M., Cohen, S., and Bielling, K.: The kinetic isotope effect for carbon and oxygen in the reaction  $\text{CO} + \text{OH}$ , *Int. J. Chem. Kinet.*, 12, 935-948, 10.1002/kin.550121205, 1980.
- Stevens, C. M., and Krout, L.: Method for the Determination of the Concentration and of the Carbon and Oxygen Isotopic Composition of Atmospheric Carbon Monoxide, *International Journal of Mass Spectrometry and Ion Physics*, 8, 265-275, 1972.
- Stevens, C. M., Krout, L., Walling, D., and Venters, A.: The Isotopic Composition of Atmospheric Carbon Monoxide, *Earth and Planetary Science Letters*, 16, 147-165, 1972.
- Stevens, C. M., and Wagner, A. F.: The role of isotope fractionation effects in atmospheric chemistry, *Z. Naturforsch. Sect. A-J. Phys. Sci.*, 44, 376-384, 1989.

- Strode, S. A., Liu, J. H., Lait, L., Commane, R., Daube, B., Wofsy, S., Conaty, A., Newman, P., and Prather, M.: Forecasting carbon monoxide on a global scale for the ATom-1 aircraft mission: insights from airborne and satellite observations and modeling, *Atmospheric Chemistry and Physics*, 18, 10955-10971, 10.5194/acp-18-10955-2018, 2018.
- Stuiver, M., and Polach, H. A.: Reporting of C-14 data - discussion, *Radiocarbon*, 19, 355-363, 1977.
- Turnbull, J., Guenther, D., Karion, A., Sweeney, C., Anderson, E., Andrews, A., Kofler, J., Miles, N., Newberger, T., and Richardson, S.: An integrated flask sample collection system for greenhouse gas measurements, *Atmospheric Measurement Techniques*, 5, 2321-2327, 2012.
- Turnbull, J. C., Karion, A., Davis, K. J., Lauvaux, T., Miles, N. L., Richardson, S. J., Sweeney, C., McKain, K., Lehman, S. J., Gurney, K. R., Patarasuk, R., Liang, J. M., Shepson, P. B., Heimburger, A., Harvey, R., and Whetstone, J.: Synthesis of Urban CO<sub>2</sub> Emission Estimates from Multiple Methods from the Indianapolis Flux Project (INFLUX), *Environ. Sci. Technol.*, 53, 287-295, 10.1021/acs.est.8b05552, 2019.
- Turnbull, J. C., Miller, J. B., Lehman, S. J., Tans, P. P., Sparks, R. J., and Southon, J.: Comparison of <sup>14</sup>CO<sub>2</sub>, CO, and SF<sub>6</sub> as tracers for recently added fossil fuel CO<sub>2</sub> in the atmosphere and implications for biological CO<sub>2</sub> exchange, *Geophysical Research Letters*, 33, 10.1029/2005gl024213, 2006.
- Turnbull, J. C., Sweeney, C., Karion, A., Newberger, T., Lehman, S. J., Tans, P. P., Davis, K. J., Lauvaux, T., Miles, N. L., and Richardson, S. J.: Toward quantification and source sector identification of fossil fuel CO<sub>2</sub> emissions from an urban area: Results from the INFLUX experiment, *Journal of Geophysical Research: Atmospheres*, 2015.
- Vimont, I. J., Turnbull, J. C., Petrenko, V. V., Place, P. F., Karion, A., Miles, N. L., Richardson, S. J., Gurney, K. R., Patarasuk, R., Sweeney, C., Vaughn, B., and White, J. W. C.: Carbon monoxide isotopic measurements in Indianapolis constrain urban source isotopic signatures and support mobile fossil fuel emissions as the dominant wintertime CO source, *Elem Sci Anth*, 5, 10.1525/elementa.136, 2017.
- Zhou, Y., Mao, H., Demerjian, K., Hogrefe, C., and Liu, J.: Regional and hemispheric influences on temporal variability in baseline carbon monoxide and ozone over the Northeast US, *Atmospheric Environment*, 164, 309-324, 10.1016/j.atmosenv.2017.06.017, 2017.
- Zobitz, J. M., Keener, J. P., Schnyder, H., and Bowling, D. R.: Sensitivity analysis and quantification of uncertainty for isotopic mixing relationships in carbon cycle research, *Agric. For. Meteorol.*, 136, 56-75, 10.1016/j.agrformet.2006.01.003, 2006.

## Figures and Tables

**Table 1:** The four main CO sources and the OH sink listed with their isotopic signatures and uncertainties.

Isotopic Sources and Sinks				
Source/Sink	$\delta^{13}\text{C}$ (VPDB)	Uncertainty	$\delta^{18}\text{O}$ (VSMOW)	Uncertainty
<b>Global Sources</b>				
Fossil Fuel Combustion <sup>a,b</sup>	-27.5‰	≤1‰	23.5‰	≤1‰
Biomass Burning <sup>c,d,e,f,*</sup>	-12-25‰	1-3‰	10-18‰	1-3‰
CH <sub>4</sub> Oxidation <sup>f,g</sup>	-52.6‰	1-3‰	0‰	>3‰
VOC Oxidation (prior estimates) <sup>c,g</sup>	-32‰	1-3‰	0‰	>3‰
<b>VOC Oxidation (this study)</b>	<b>-32.8‰</b>	<b>0.5‰</b>	<b>3.6‰</b>	<b>1.2‰</b>
CO Oxidation by OH Fractionation Factors <sup>**</sup>	~ 5‰	-3‰ – +6‰	~-10‰	-11‰ – -9‰

<sup>a</sup> Stevens et al. (1972)

<sup>b</sup> Brenninkmeijer (1993)

<sup>c</sup> Stevens and Wagner (1989)

<sup>d</sup> Bergamaschi et al. (1998)

<sup>e</sup> Saurer et al. (2009)

<sup>f</sup> Manning et al. (1997)

<sup>g</sup> Brenninkmeijer and Röckmann (1997)

\* Isotopic signatures vary based on type of vegetation burned (C3/C4) and temperature of fire

\*\* These factors are the "best estimate" provided Brenninkmeijer et al. (1999). These are based on data from Röckmann et al. (1998), and Stevens et al. (1980). These studies report pressure dependent fractionation factors for  $\epsilon^{13}\text{C}$  and very little pressure dependence for  $\epsilon^{18}\text{O}$  (pressure range ~200 mbar to 1100 mbar). The variability in the fractionation factors is reported here as the uncertainty.

**Table 2:** VOC signature calculation table using data from Indianapolis, IN, USA.  $\Delta^{14}\text{CO}_2$  and  $X_{\text{CO}_2\text{-FF}}$  values reported from Turnbull et al. (2015,2018).  $X_{\text{CO-ENH}}$   $1\sigma$  uncertainty is  $\pm 0.7$  nmol:mol,  $\Delta^{14}\text{CO}_2$   $1\sigma$  uncertainty is  $\sim\pm 1.8\text{‰}$  (Turnbull et al., 2015,2018), and  $X_{\text{CO}_2\text{-FF}}$   $1\sigma$  uncertainty is  $\pm 1$   $\mu\text{mol:mol}$  (Turnbull et al., 2015,2018).

Date	$X_{\text{CO-ENH}}$ (nmol:mol)	$\Delta^{14}\text{CO}_2$ (‰)	$X_{\text{CO}_2\text{-FF}}$ ( $\mu\text{mol:mol}$ )	$X_{\text{CO-FF}}$ (nmol:mol)	$X_{\text{CO-VOC}}$ (nmol:mol)	$\delta^{13}\text{C}_{\text{VOC}}$ (‰)	$\delta^{18}\text{O}_{\text{VOC}}$ (‰)
5/5/15	11.1	10.6	0.7	5.1	6.0	-31.2	8.0
5/12/14	9.5	17.4	0.6	4.0	5.5	-31.0	8.6
5/28/14	12.5	14.6	0.8	5.9	6.6	-31.2	7.8
6/8/15	38.7	9.4	3.2	22.2	16.6	-32.1	5.5
6/30/15	12.7	12.5	1.3	8.9	3.8	-34.0	0.1
6/3/14	13.2	18.0	1.4	9.6	3.7	-34.5	-1.1
7/27/13	19.9	22.7	1.9	13.1	6.8	-33.2	2.4
8/1/13	12.3	26.1	1.3	9.4	2.9	-35.6	-4.4
8/20/14	9.8	16.1	0.8	5.3	4.5	-31.8	6.3
8/12/14	25.0	17.7	2.6	18.1	6.9	-34.5	-1.3
8/21/14	27.1	9.6	2.6	17.9	9.2	-33.2	2.4
9/2/14	25.6	12.6	1.4	9.9	15.7	-30.8	9.2

**Figure 1:** Satellite Image of INFLUX tower locations. Arrow indicates predominant wind direction during sampling. Samples from this study were taken from towers 1 and 2 (shown). Also note the vegetation cover between the two towers.

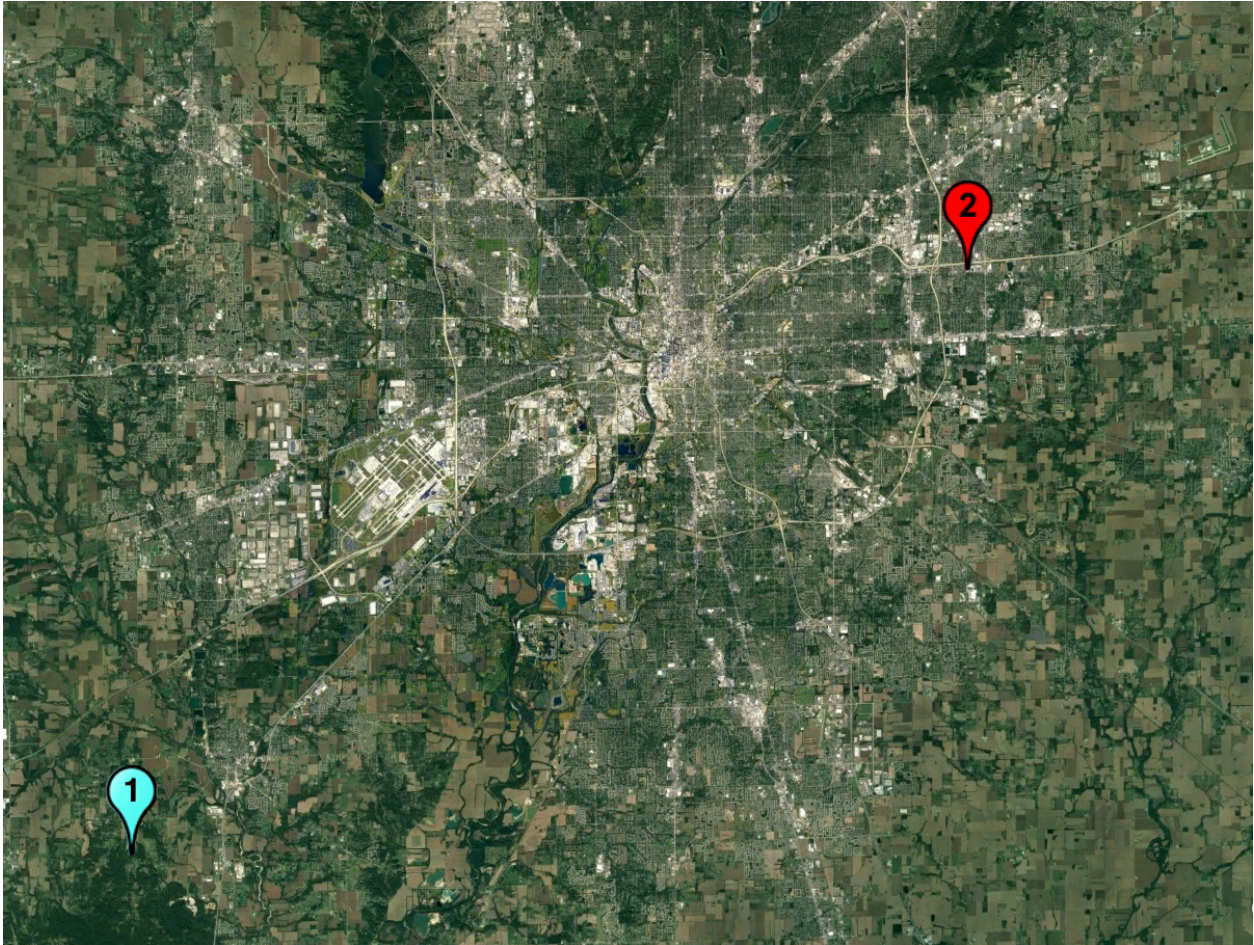
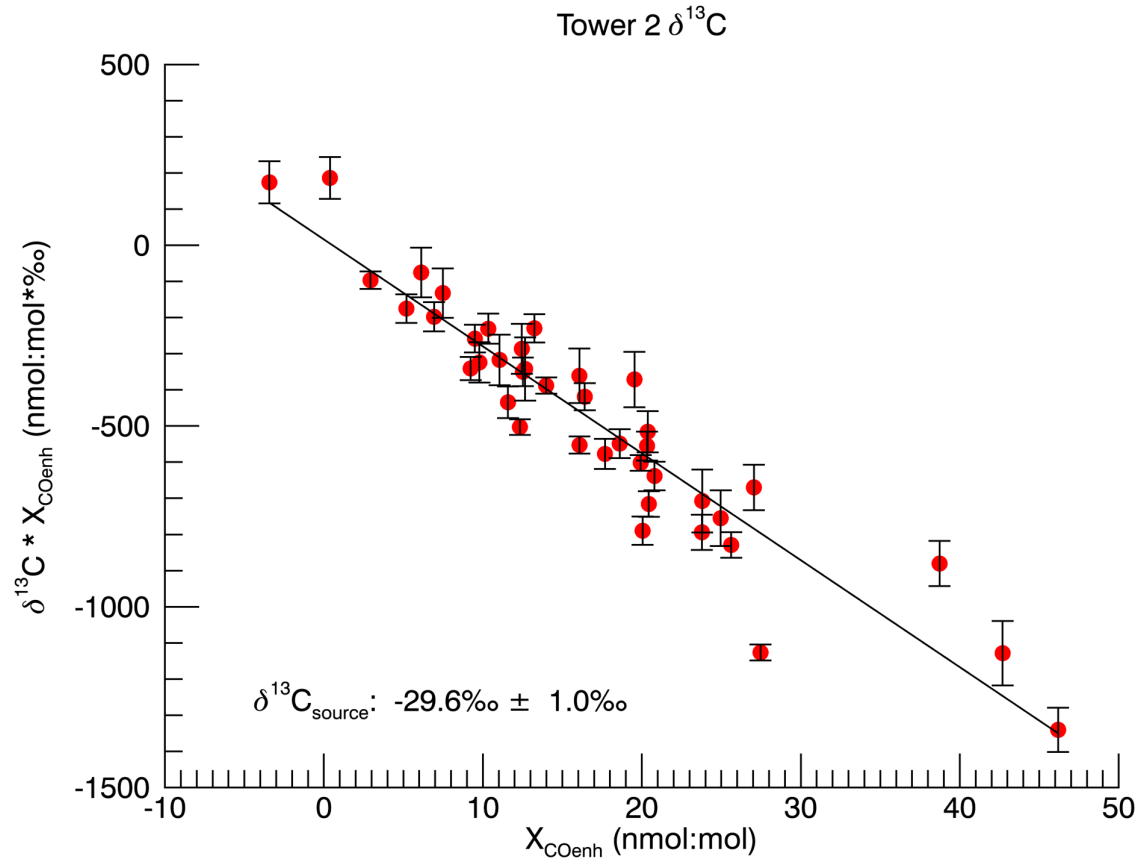


**Figure 2:** Indianapolis Miller Tans plots for late spring through summer (May, June, July, August, September). The error bars represent the propagated error for the calculation of the enhancements (see text for details).



Tower 2  $\delta^{18}\text{O}$

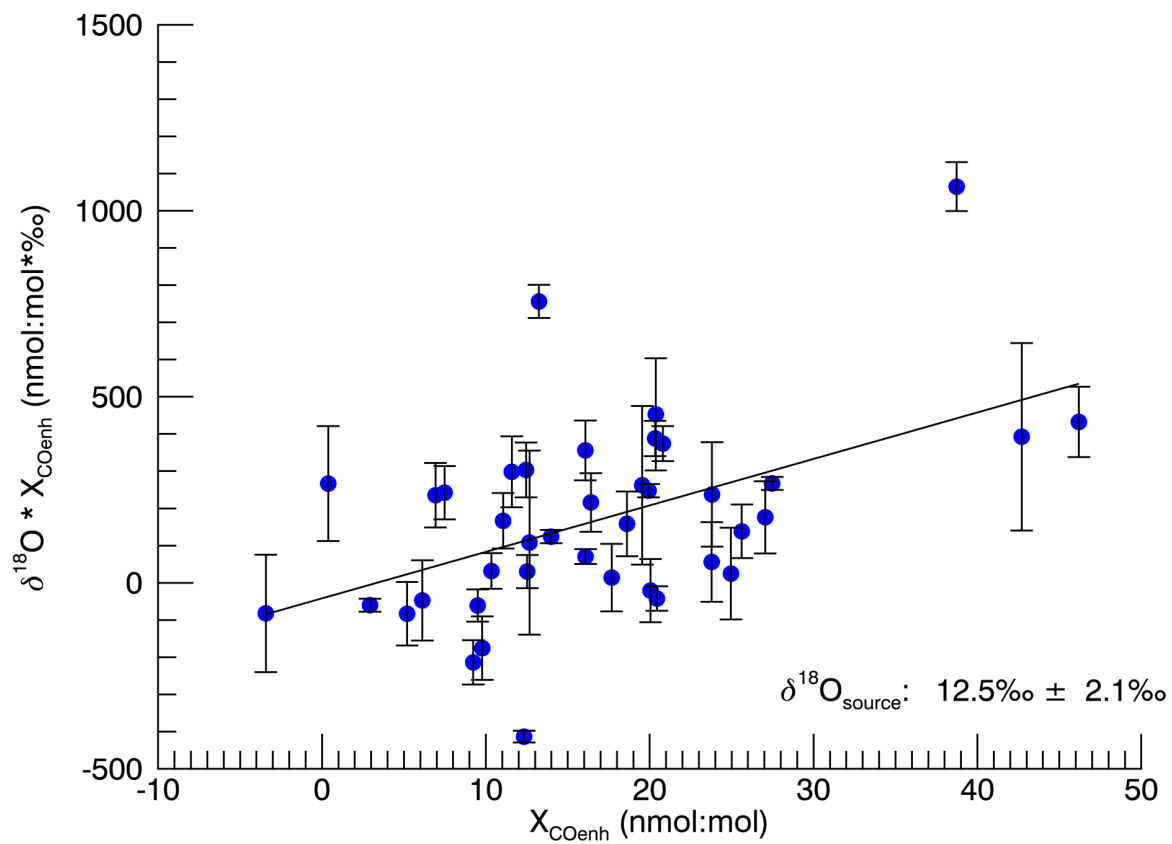


**Figure 3:** Time series of towers 1 and 2 at Indianapolis. These data were previously shown in Vimont et al. (2017), but are reproduced here for the convenience of the reader. The curves shown are for sighting purposes only. They are a simple single harmonic polynomial smoothing and are meant to aid the reader in viewing the seasonal variability. The error bars represent  $1\sigma$  uncertainty. CO mole fraction  $1\sigma$  uncertainty is  $\pm 0.5$  nmol:mol. The red arrows indicate the time periods used in this study, and these data, along with  $\delta^{13}\text{C}$  and  $\delta^{18}\text{O}$   $1\sigma$  uncertainty is listed in the supplementary material (Table S2).

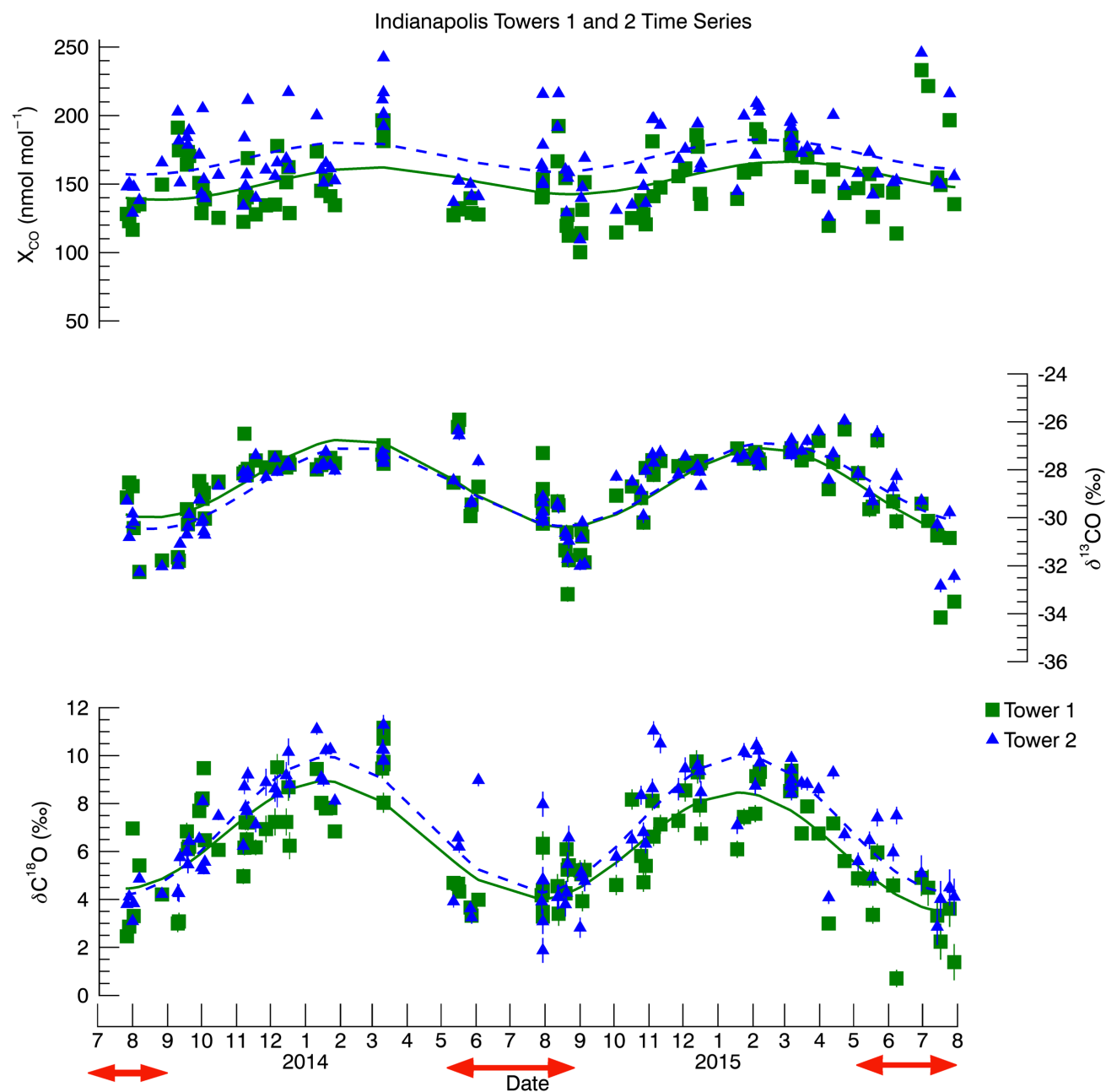


**Figure 4:** Time series for Beech Island, South Carolina. No curves were fit to the data due to the short time frame for the measurements. The error bars represent  $1\sigma$  analytical uncertainty. CO mole fraction  $1\sigma$  uncertainty is  $\pm 0.5$  nmol:mol. Uncertainty for  $\delta^{13}\text{C}$  and  $\delta^{18}\text{O}$  is listed in the supplementary material (Table S3). The CO mole fraction data are taken from the NOAA GGGRN dataset (Andrews et al., 2009). The green and blue arrows indicate the summer and winter periods used in this study, respectively.

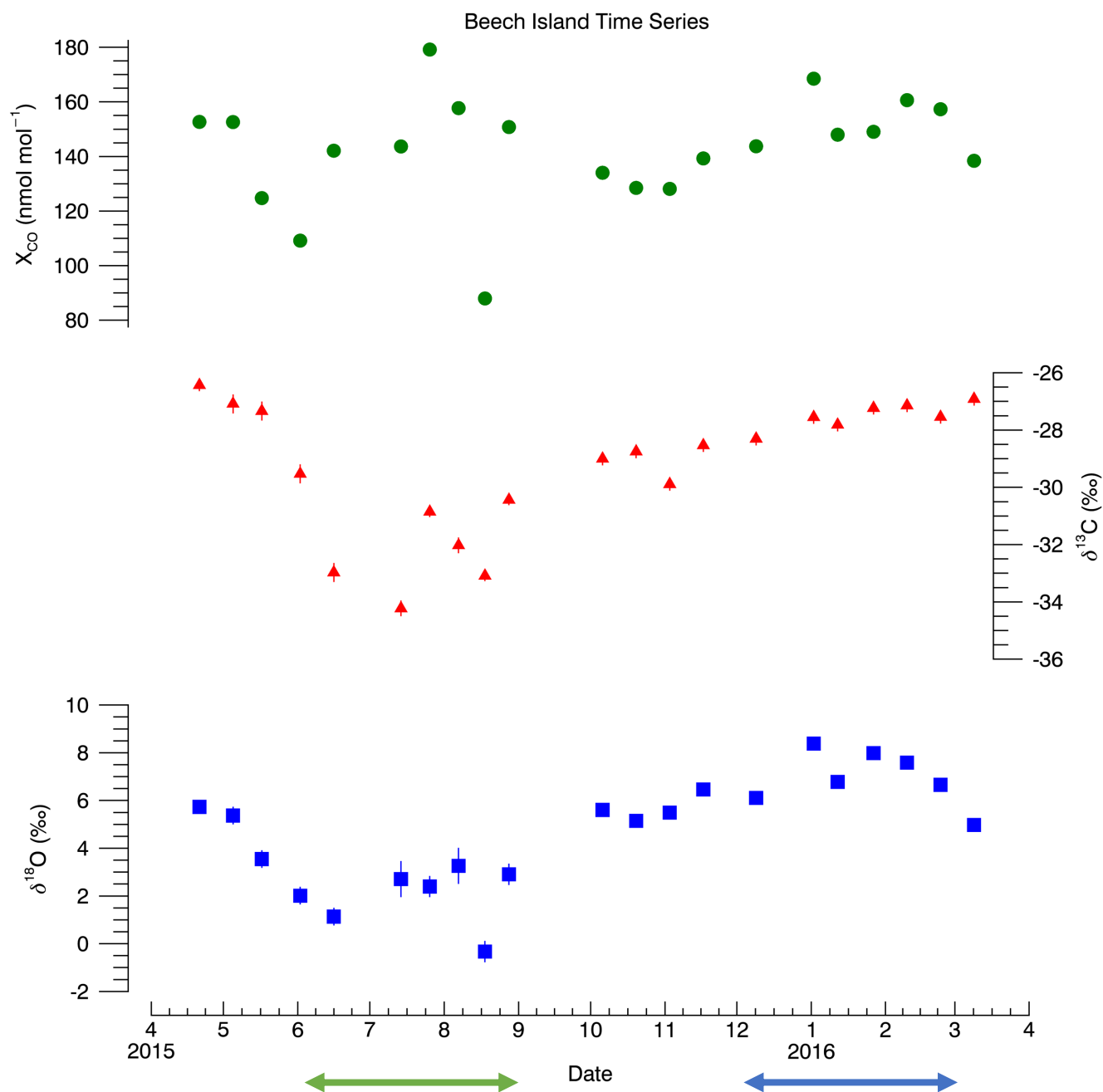
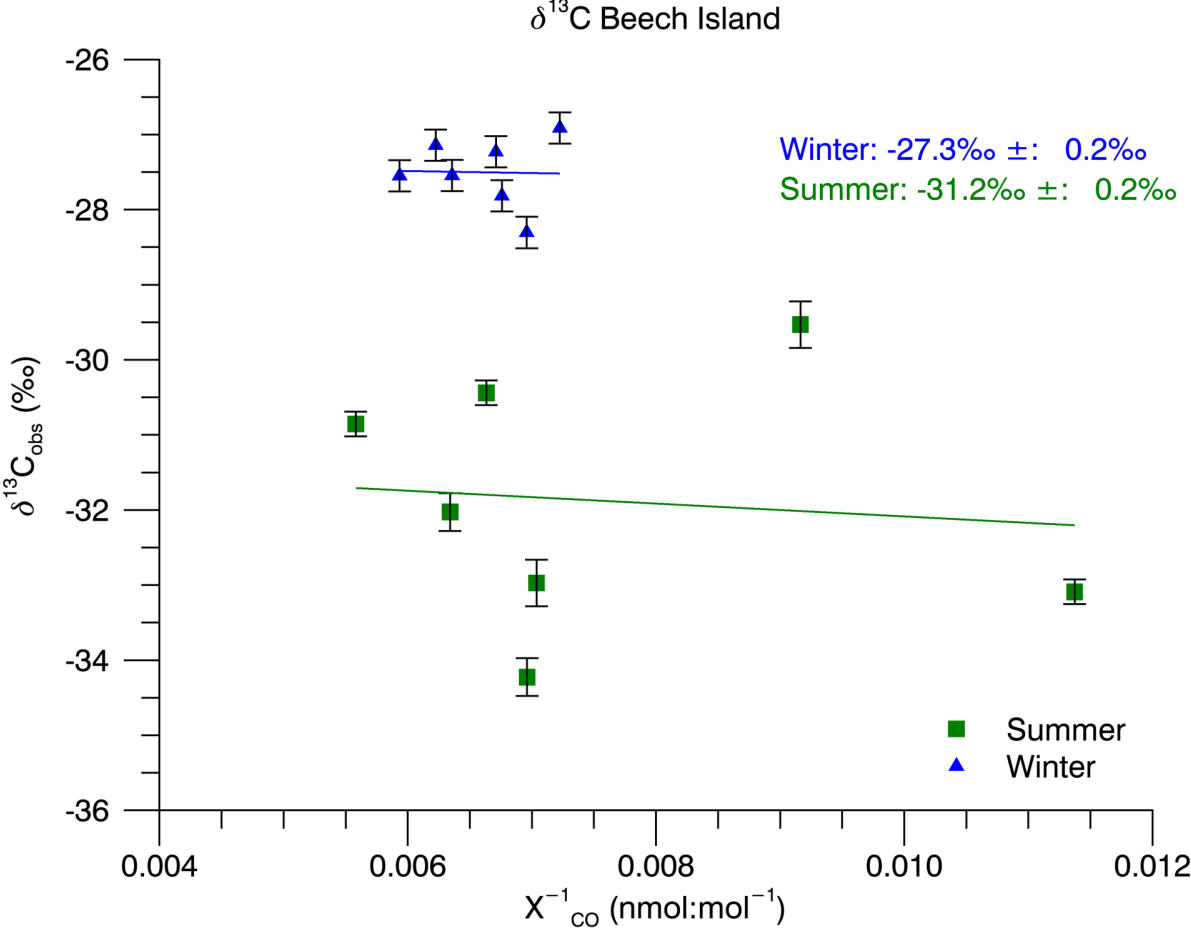


**Figure 5:** Beech Island Keeling plots. The reported intercepts and uncertainties are the standard Monte Carlo simulation results. We also performed a bootstrap Monte Carlo. Those results are reported in the text.



$\delta^{18}\text{O}$  Beech Island

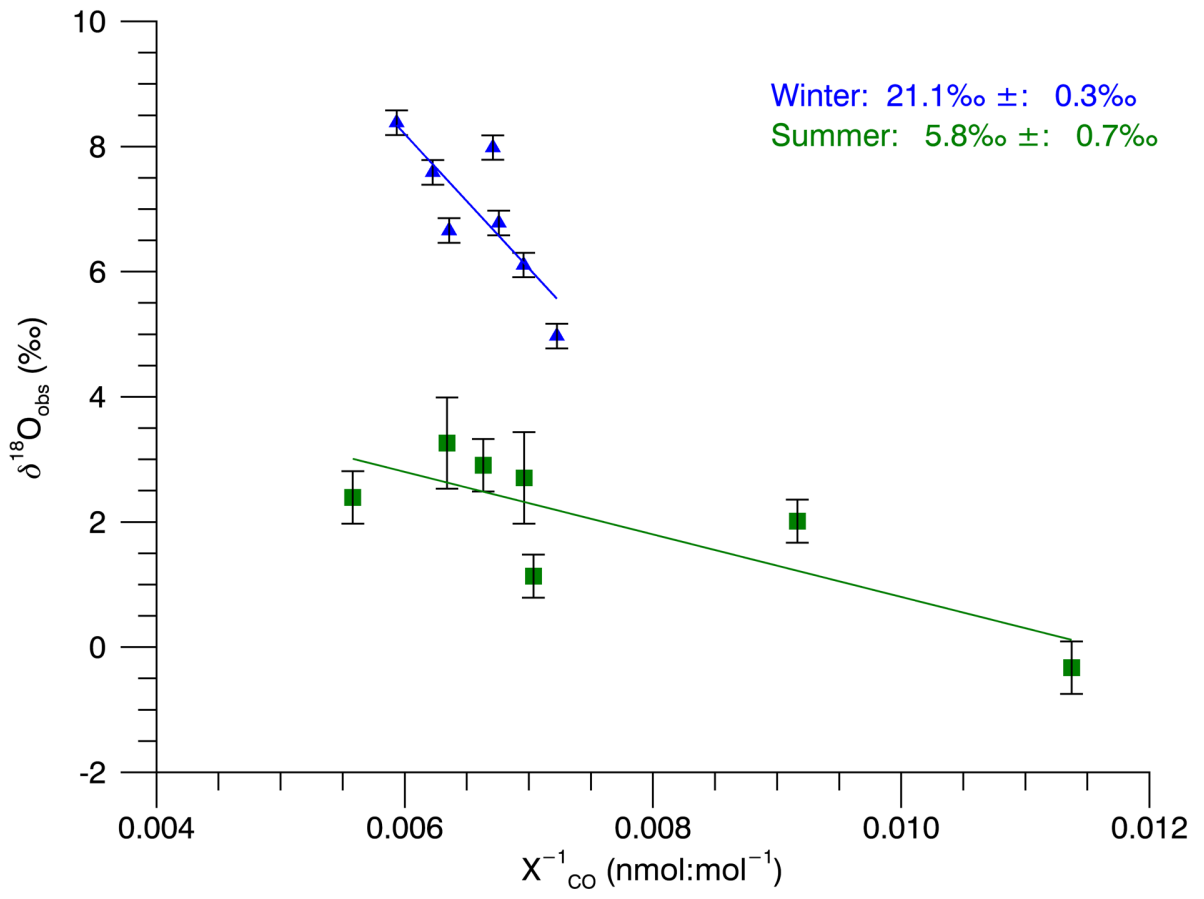


**Figure 6:** Miller Tans Analysis of Beech Island seasonal source signatures using monthly means from Izaña, Tennerife (Bräunlich, 2000). Green squares indicate summer data, blue triangles indicate winter data. The  $\delta^{13}\text{C}$  and  $\delta^{18}\text{O}$  values reported are the mean of 10,000 regression slopes from our Monte Carlo simulation (section 2.5). The uncertainty is the standard deviation of the 10,000 slopes.

